Improving Durability of Turbine Components Through Trenched Film Cooling and Contoured Endwalls

DOE Award Number DE-FE0005540
UTSR Project Number 07-01-SR127

Principal Investigator:
Prof. David G. Bogard
Todd Davidson and David Kistenmacher
University of Texas at Austin

Co-Principal Investigator:
Prof. Karen A. Thole
Alan Thrift and Amy Mensch
Pennsylvania State University

UTSR Peer Review Workshop VII
October 25, 2011

Background image: [Hamed, A., Tabakoff, W., and Wenglarz, R., 2006]

Project Objectives

a. Evaluate the degradation of performance for trench and crater film cooling configurations when subjected to active deposition of contaminants. This will be done on simulated vane and endwall models.

b. Design improved trench or crater film cooling configurations that mitigate the degradation effects of deposition of contaminants.

c. Determine the overall cooling effectiveness (including conjugate heat transfer effects) with and without thermal barrier coatings for the vane and endwall.

Project Objectives, continued

d. Develop the knowledge needed to design film cooling configurations on contoured endwalls.

e. Perform detailed velocity and thermal field measurements along the vane, endwall, and downstream wake, with and without film cooling, to provide benchmarks to evaluate CFD simulations.

f. Develop improved cooling designs specifically for the vane-endwall junction including mitigation of deposition effects.

Experiments were conducted to investigate effects of TBC and contaminant depositions on film cooling performance for a vane.

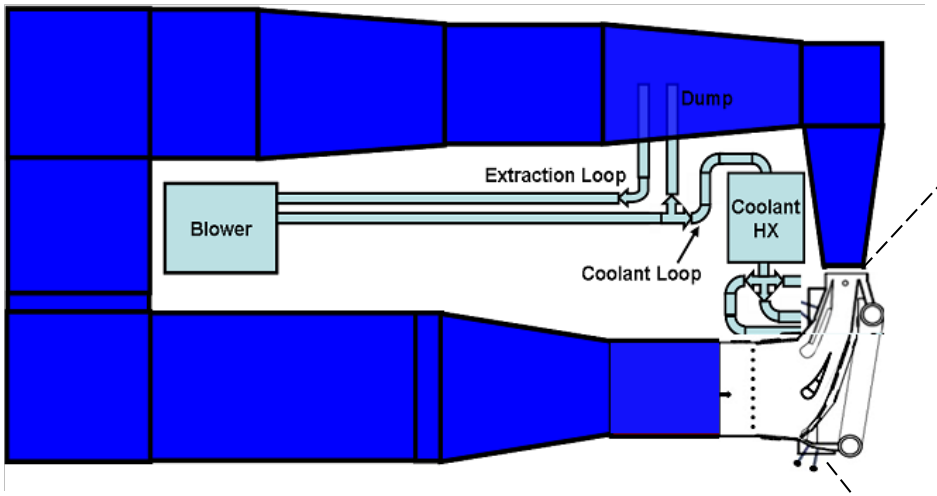

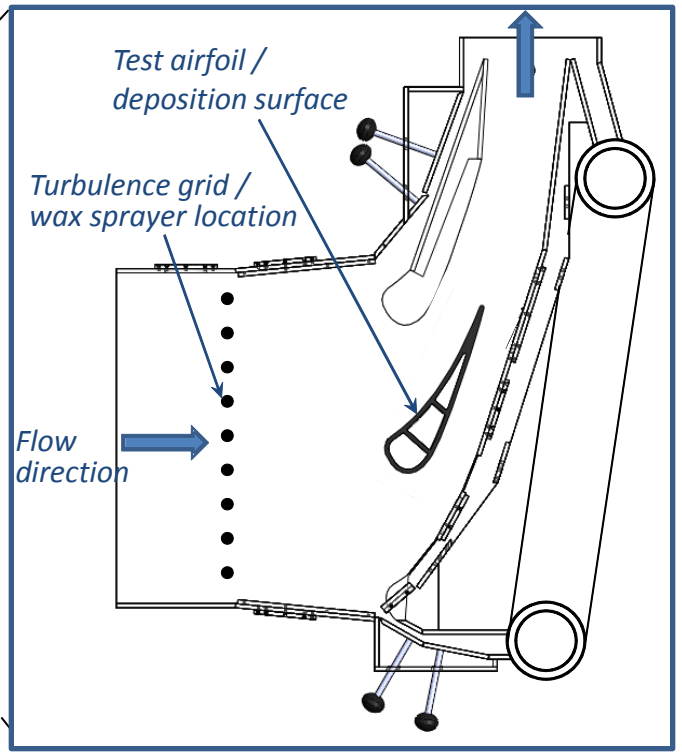

- Performance was quantified in terms of overall effectiveness.
- Multiple hole geometries were investigated.

What is the overall effectiveness?

Adiabatic effectiveness is traditionally used to quantify film performance

$$\eta = \frac{T_\infty - T_{aw}}{T_\infty - T_{c,exit}}$$

T_∞ = mainstream temperature

T_{aw} = adiabatic wall temperature

$T_{c,exit}$ = coolant temperature at the exit of the hole

The "overall effectiveness", ϕ, is obtained using a conducting model and is defined as follows:

$$\phi = \frac{T_\infty - T_m}{T_\infty - T_c}$$

where:

T_m = "metal" temperature

T_∞ = mainstream temperature

T_c = coolant temperature in the plenum

ϕ is a dimensionless surface temperature for a conducting model which takes into account conduction through the blade wall, film cooling, internal cooling, and convective cooling within coolant holes.

To achieve a properly scaled ϕ, certain parameters must be matched

A simplified 1-D analysis using T_{aw} as the driving temperature shows:

$$\phi = \frac{1-\eta}{1+Bi+\frac{h_e}{h_i}} + \eta$$

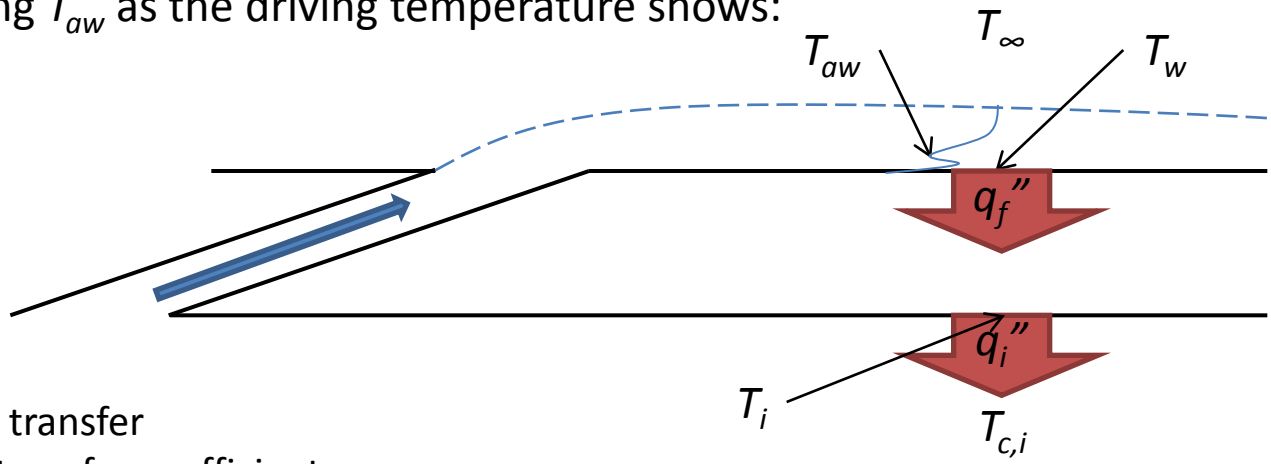

with

$$Bi = \frac{h_e t}{k}$$

h_e = external heat transfer
h_i = internal heat transfer coefficient
t = wall thickness
k = conductivity of the solid

Matched *Bi* was achieved using DuPont Corian®, k = 1.0 W/m·K

Also important to match the h_e/h_i ratio. This is done even though the magnitudes of h_e and h_i are much less than in the engine.

Of particular interest was quantification of the improved overall effectiveness due to use of TBC

- Although TBC is used extensively on actual engine hardware, there has been little experimental study because of the reliance on adiabatic effectiveness measurements.
- Trench and crater configurations can potentially be formed using TBC

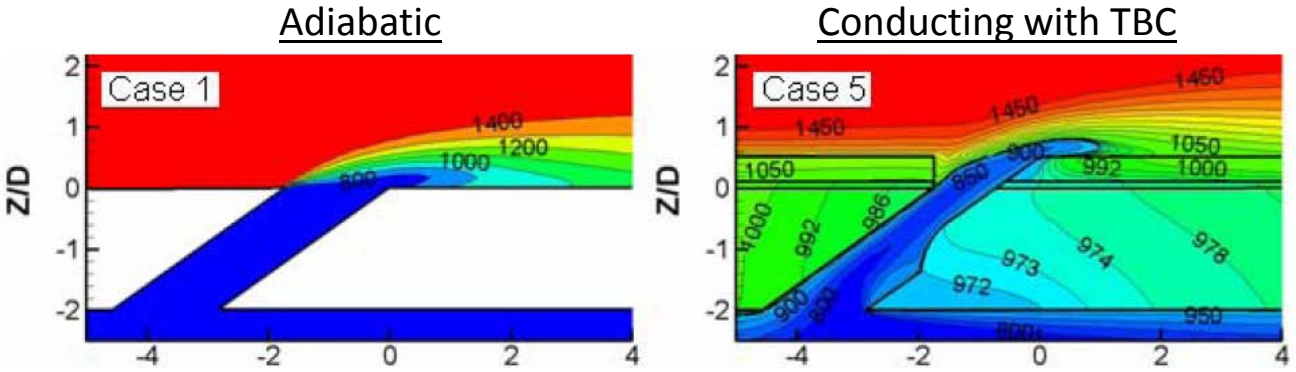

Computational study of the effects of hole blockage due to TBC (Na et al., 2007)

Overall effectiveness with TBC: $$\phi = (1 + Bi_{TBC}) \frac{1-\eta}{1 + Bi_{TBC} + Bi_{Vane} + \frac{h_e}{h_i}} + \eta$$

Distributions of overall effectiveness with no film cooling, i.e. ϕ_0, with and without TBC

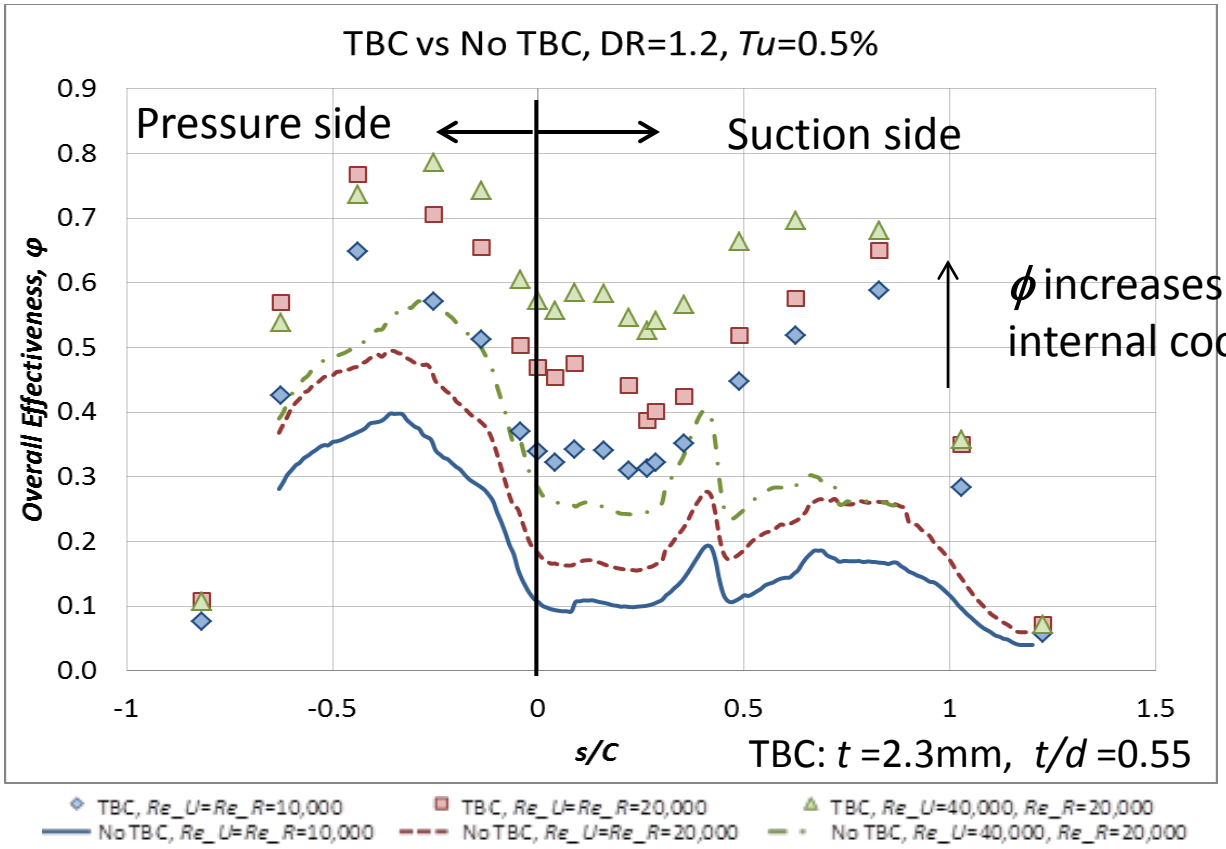

ϕ increases with increasing internal coolant flow rates

Use of TBC results in as much as a factor of 3 increase in ϕ

Film cooling configurations on suction side of the vane

- Rounds Holes
  - 24 holes
  - *s/C* = 0.23
  - *d* = 4.2 mm

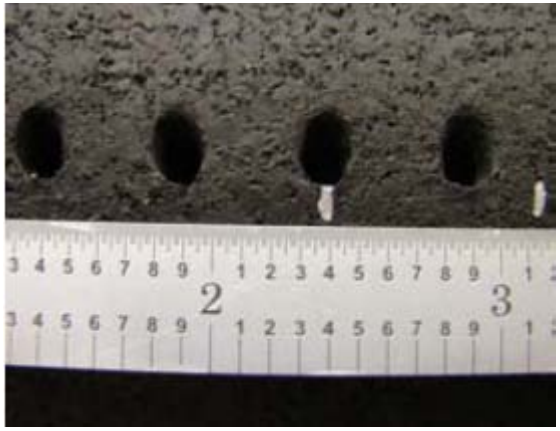

- Trench
  - Embedded round holes
  - *t/d* = 0.55 (cork thickness)
  - *w/d* = 2

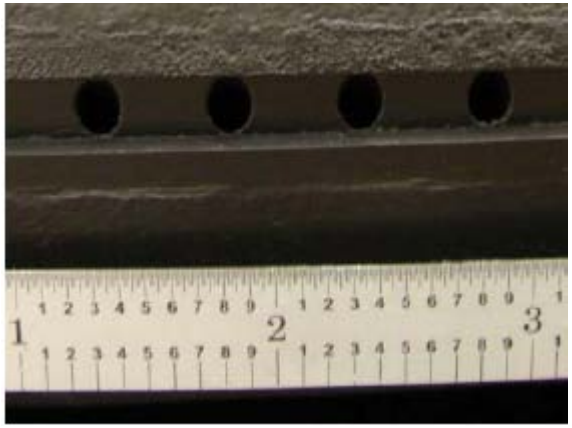

Source: Bunker, 2002

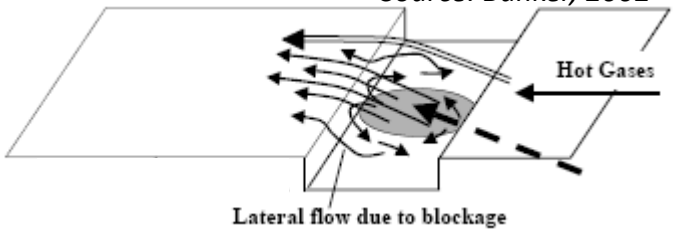

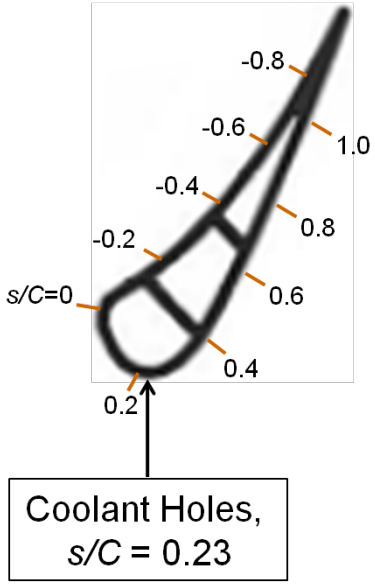

Overall effectiveness on the suction side with TBC – comparison of round and trench film cooling configurations.

Notice the upstream cooling due to convective cooling in the holes

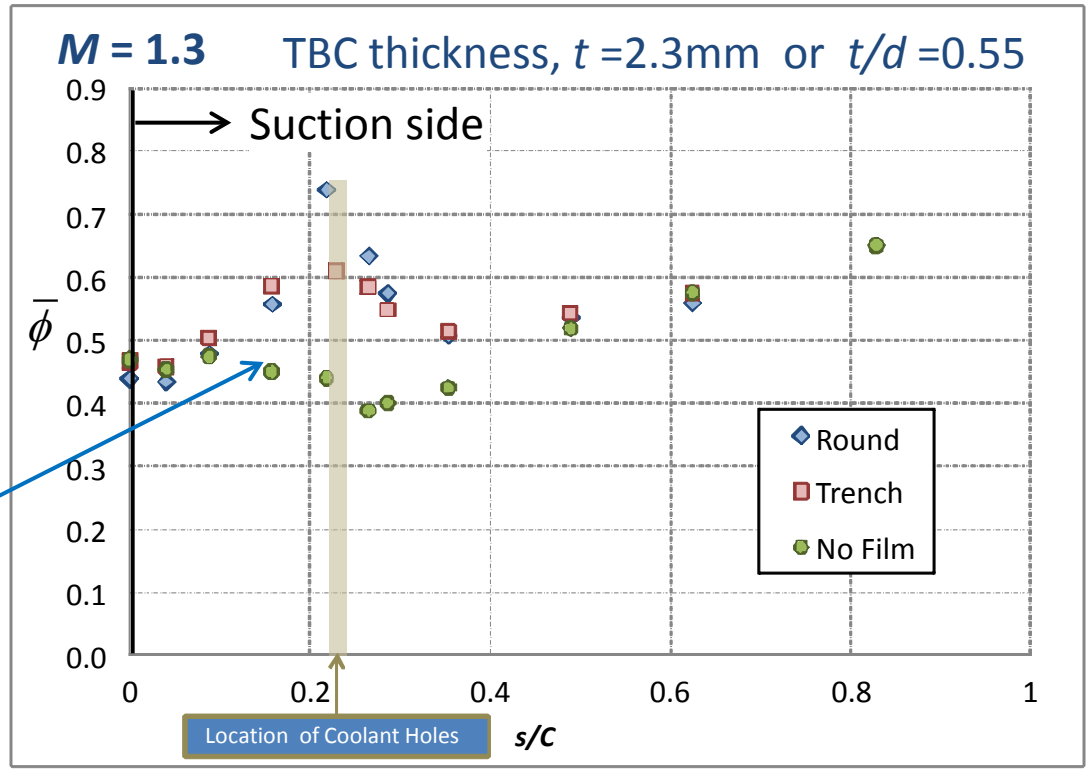

Surprisingly the trench does not show noticeable improvement, and has decreased overall effectiveness in the trench

Evaluation of predictions of ϕ based on measured values of η and ϕ_0

Prediction of overall film effectiveness using: $\phi = \phi_0(1-\eta)+\eta$

Predictions are poor near the coolant holes due to convective cooling in the holes.

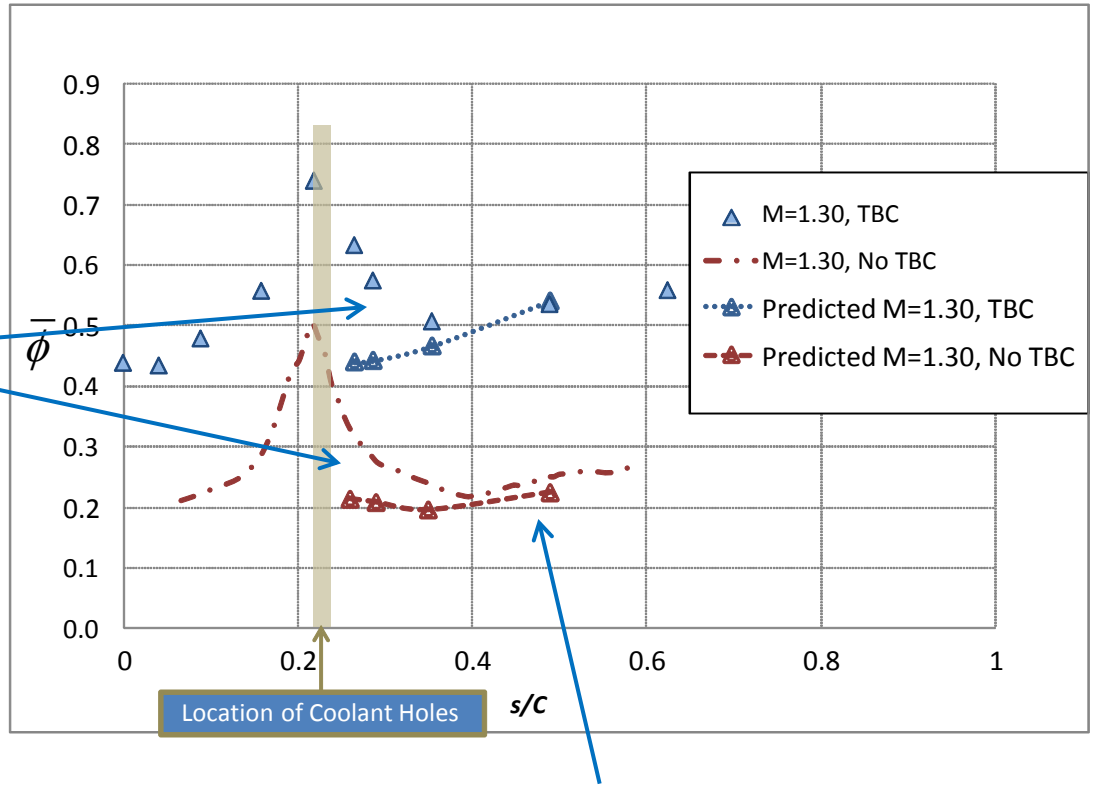

Predictions are good farther downstream

Film cooling configurations used with pressure side coolant holes

Round

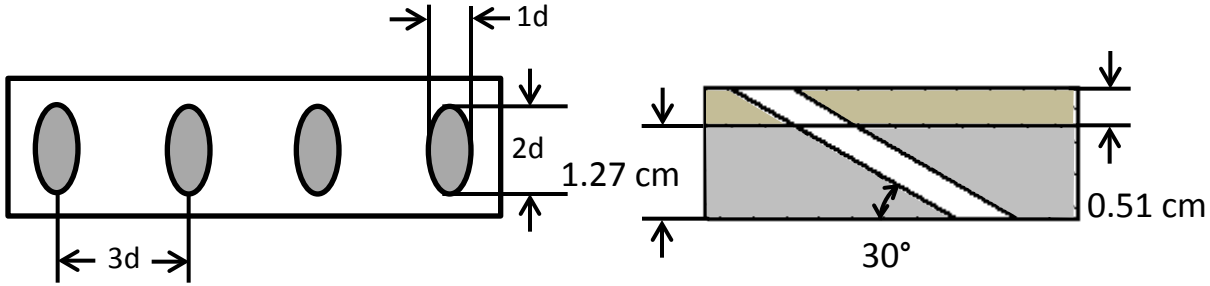

Crater

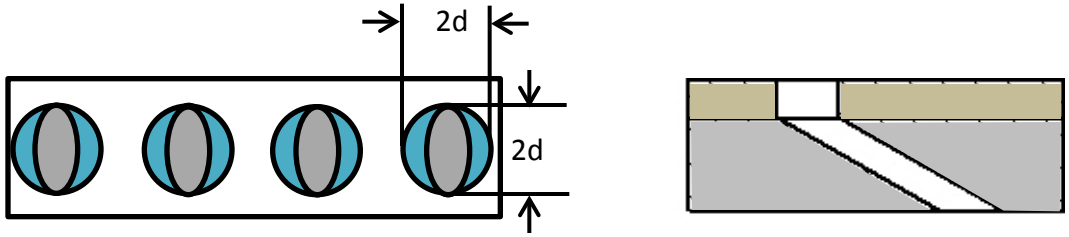

Row of holes

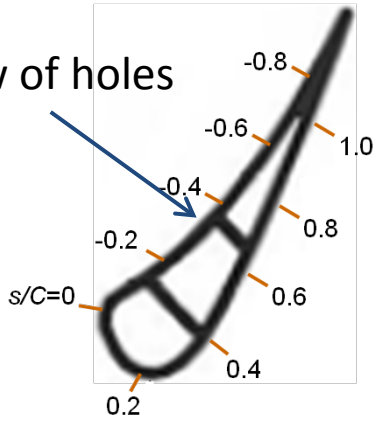

Modified trench

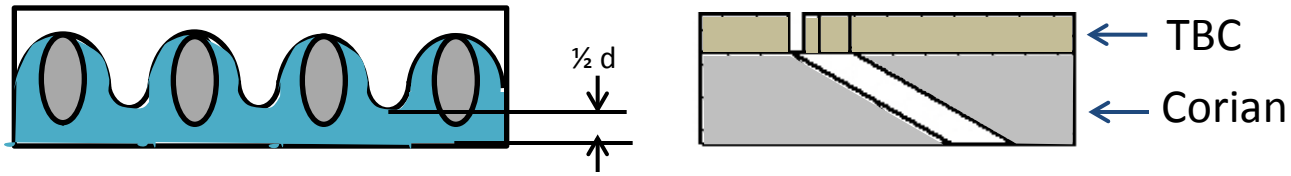

Overall effectiveness on pressure side with showerhead and PS row of holes with no TBC

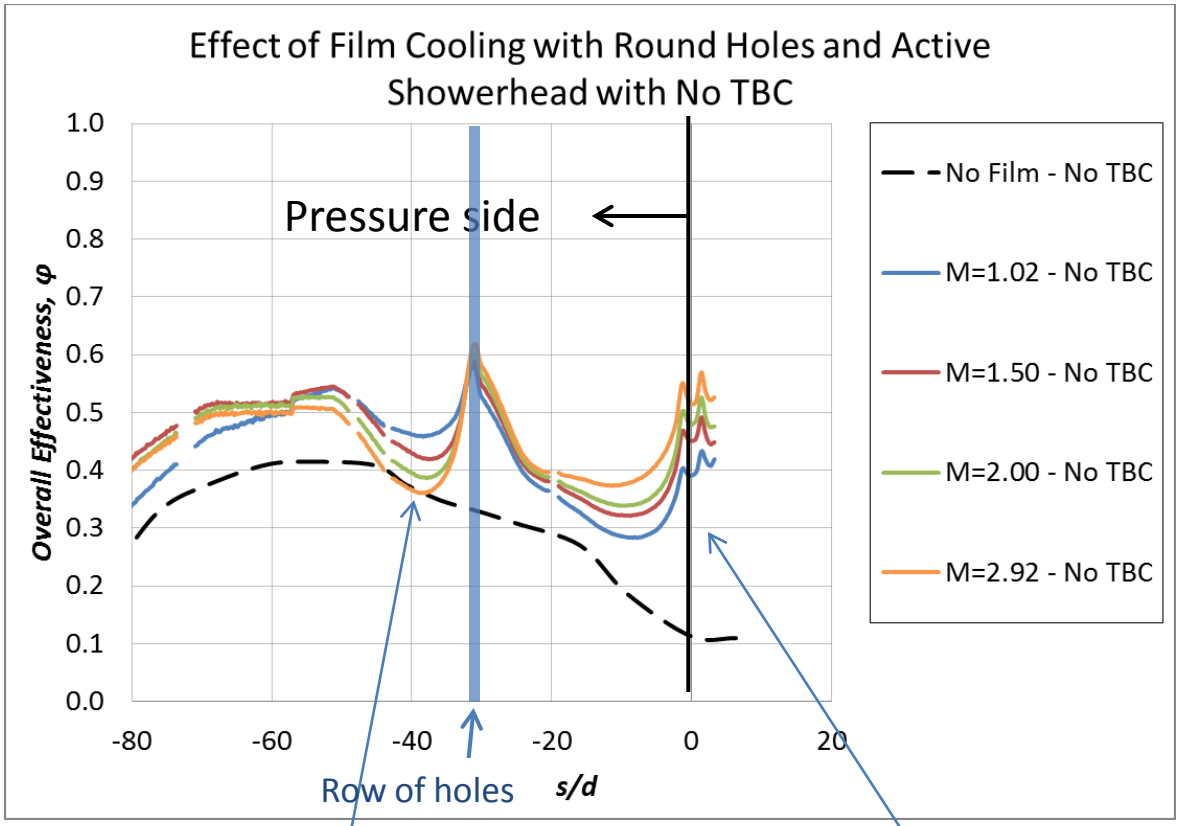

Decreasing ϕ with increasing blowing ratio downstream of pressure side holes

Increasing ϕ with increasing blowing ratio in showerhead region

Overall effectiveness on pressure side with showerhead and PS row of holes with TBC

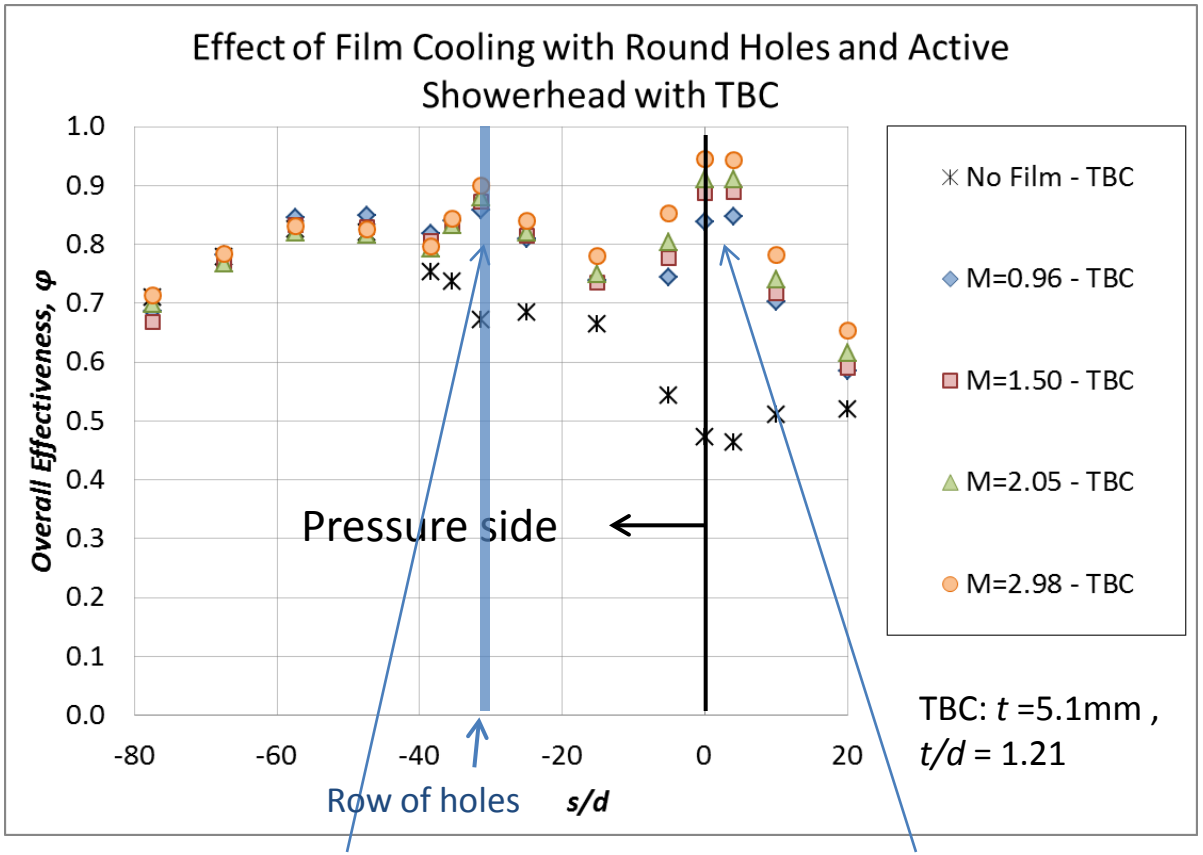

No change in ϕ with increasing blowing ratio downstream of pressure side holes

Increasing ϕ with increasing blowing ratio in showerhead region

Overall effectiveness on pressure side with showerhead and PS row of holes with and without TBC

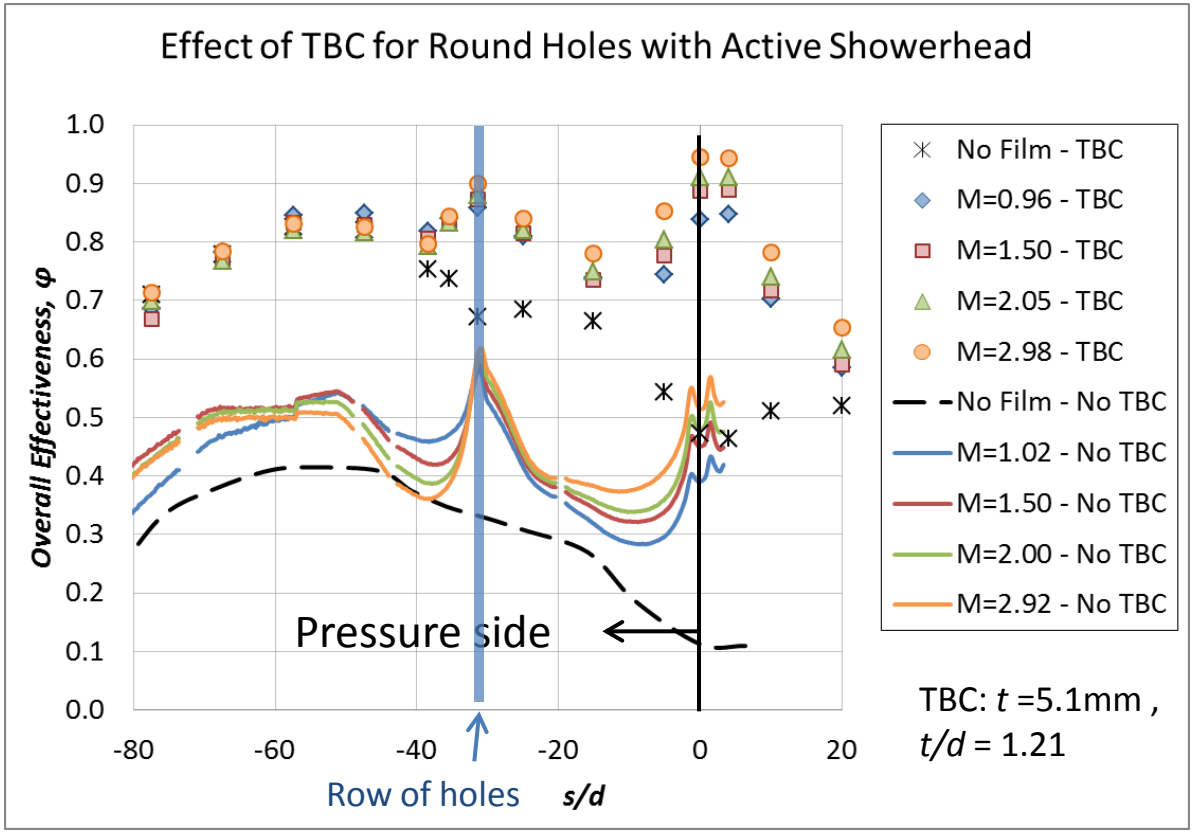

TBC has a more substantial effect than film cooling on the overall cooling effectiveness

Overall effectiveness with varying film cooling configurations with TBC

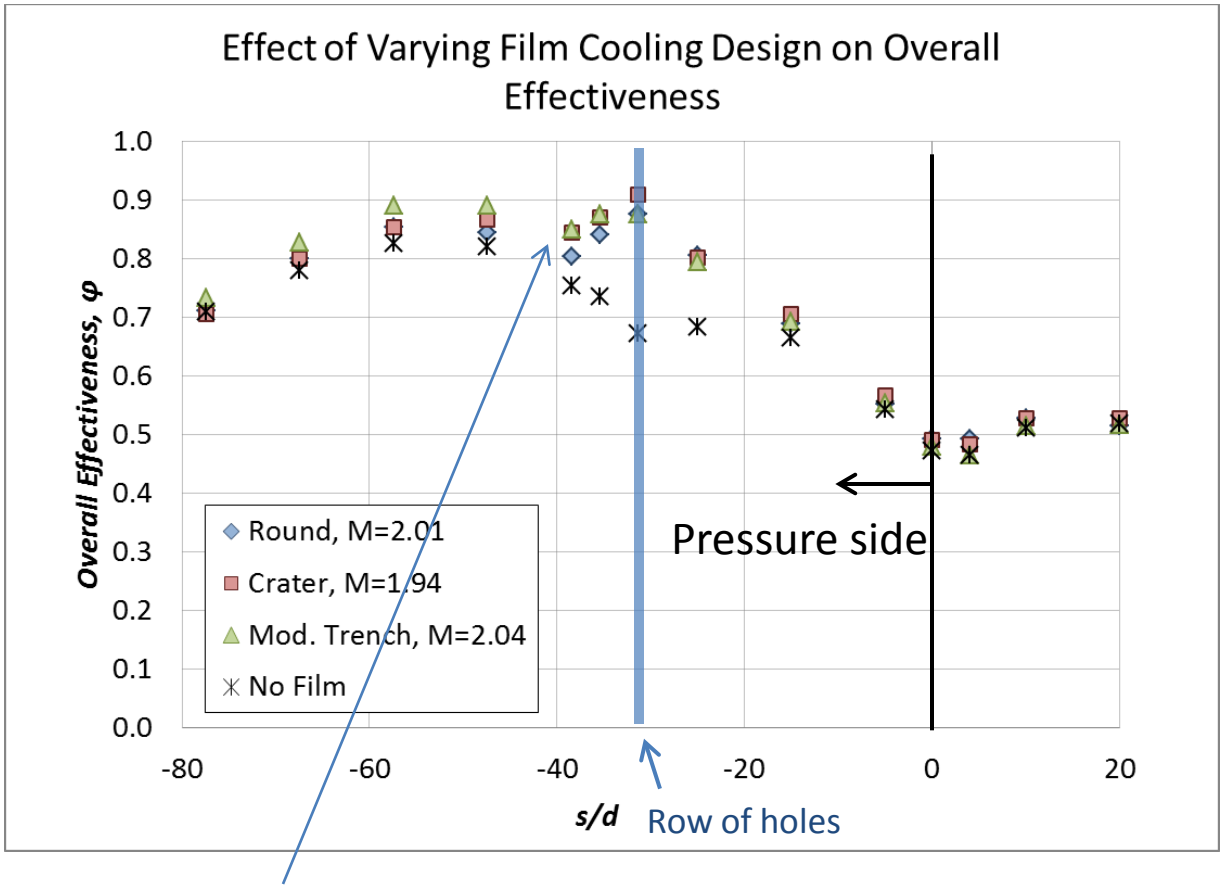

Modified trench configuration provides slightly higher overall cooling effectiveness.

Contaminant depositions simulated using wax spray technique

- Turbine depositions: Molten/softened ash particles impact and solidify on cooled airfoils and endwalls.
- This study simulates this in a wind tunnel using molten wax particles.

Schematic of the wax spray device:

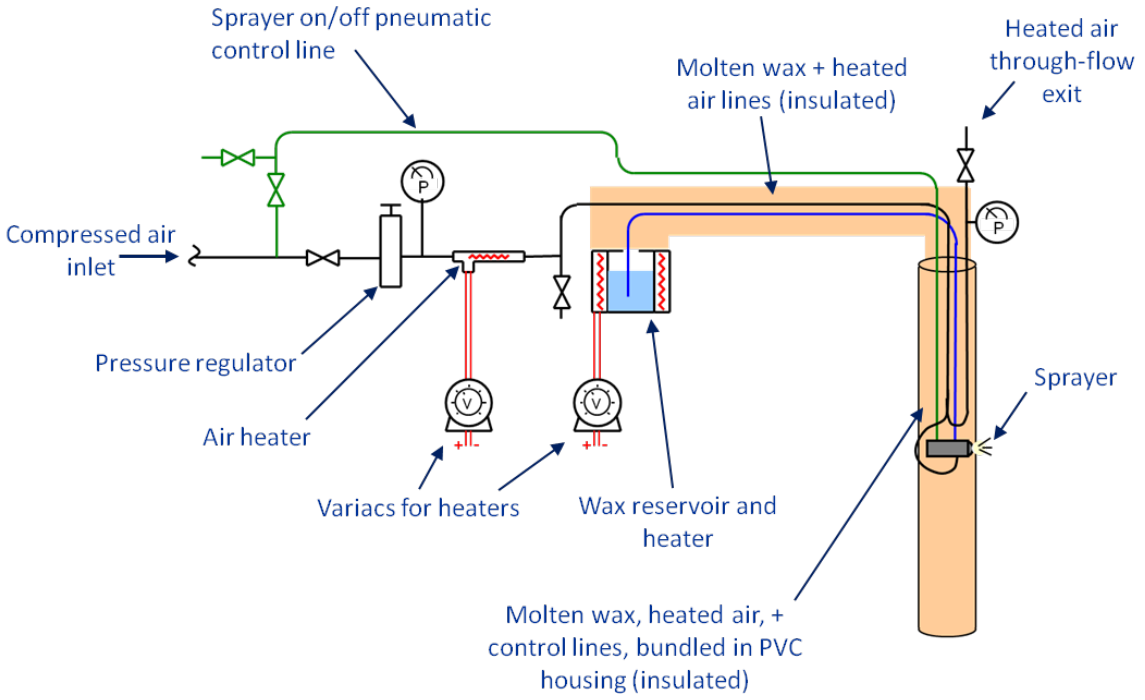

Photo of wax spray device in turbulence grid:

Images of deposition with film cooling with round holes

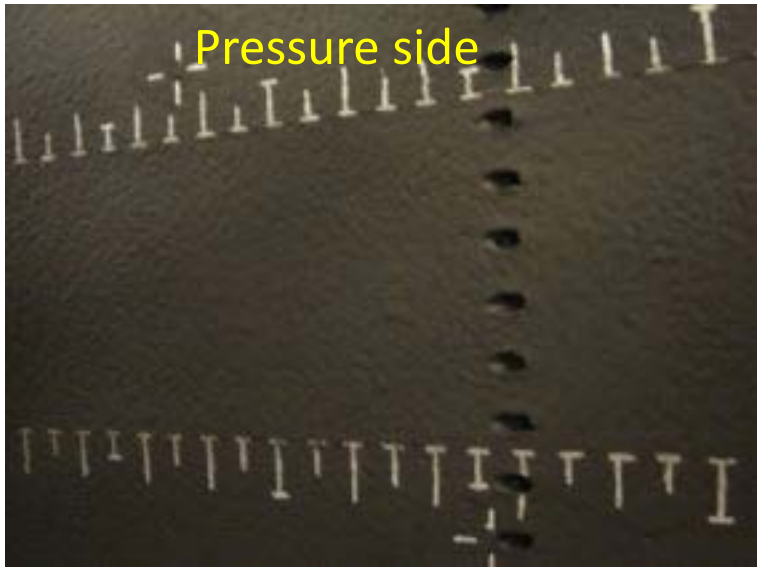

Pressure side round holes blocked by depositions

Images of deposition with film cooling with the crater configuration in TBC

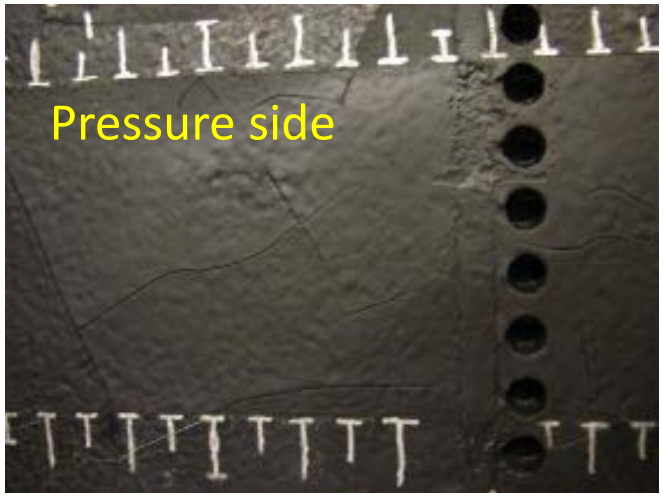

Craters are not blocked by depositions, but large buildup of depositions upstream and downstream of coolant holes.

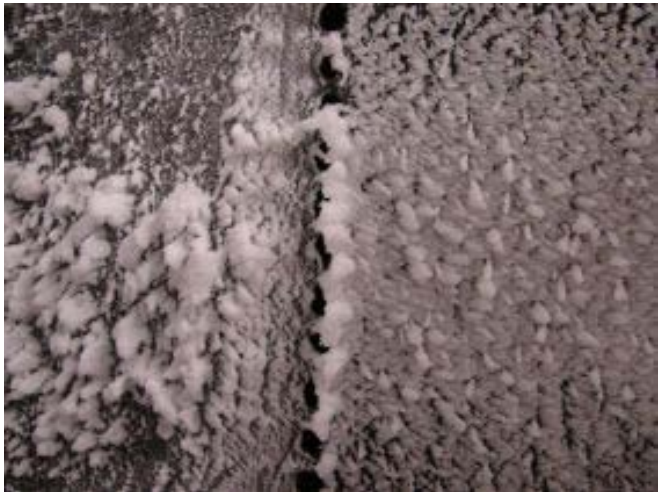

Images of deposition with film cooling with the modified trench configuration in TBC

Again, holes are not blocked by depositions, but large buildup of depositions upstream and downstream of coolant holes.

Appears that coolant interaction with molten particles has stimulated growth of depositions

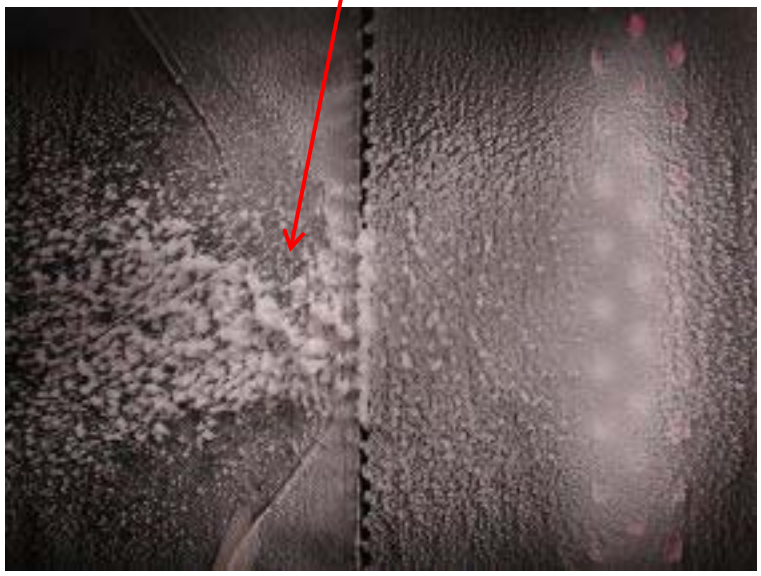

Effect of depositions on overall cooling effectiveness for a film cooled vane with TBC

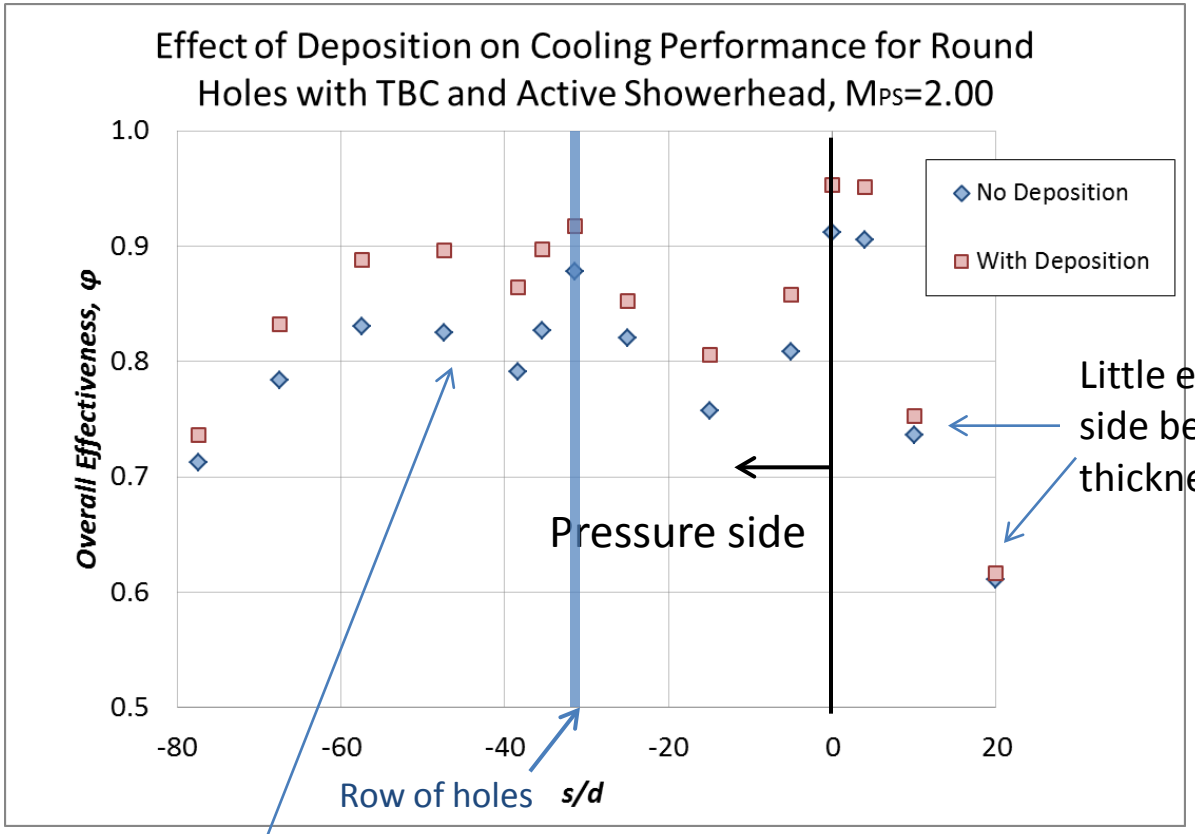

Little effect on the suction side because deposition thickness is small

Depositions cause an increase in overall cooling effectiveness!

A range of interface slot geometries were evaluated in the large scale, closed loop wind tunnel at PSU

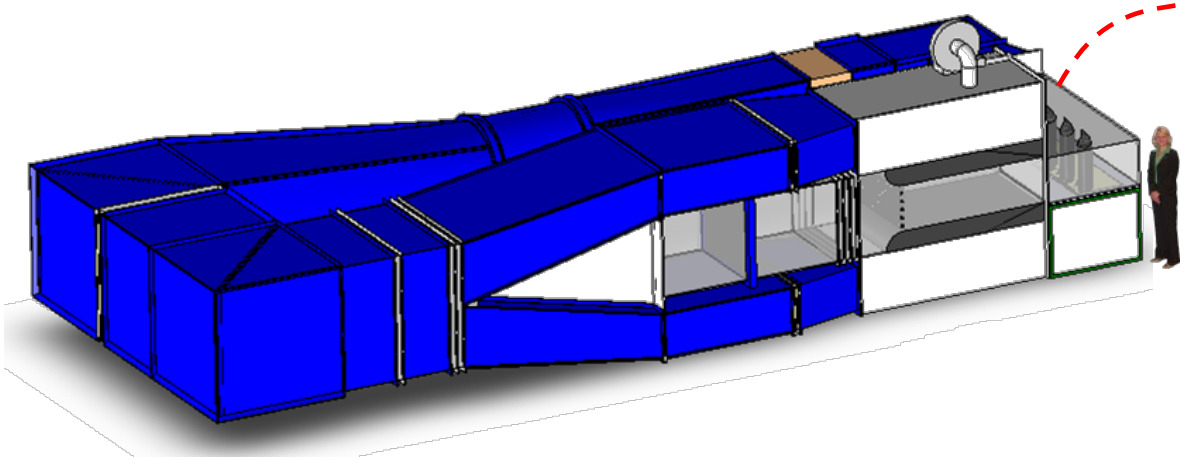

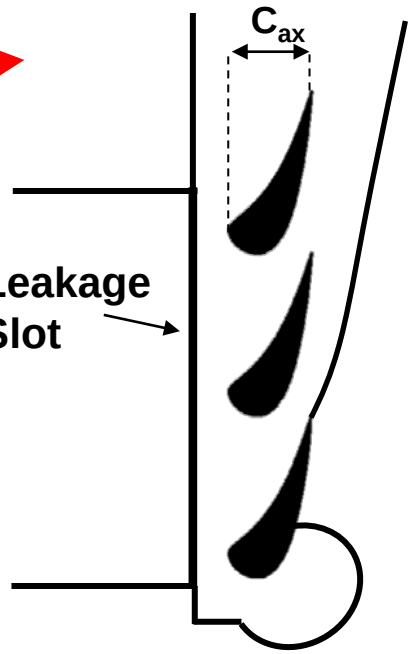

Slot Geometries

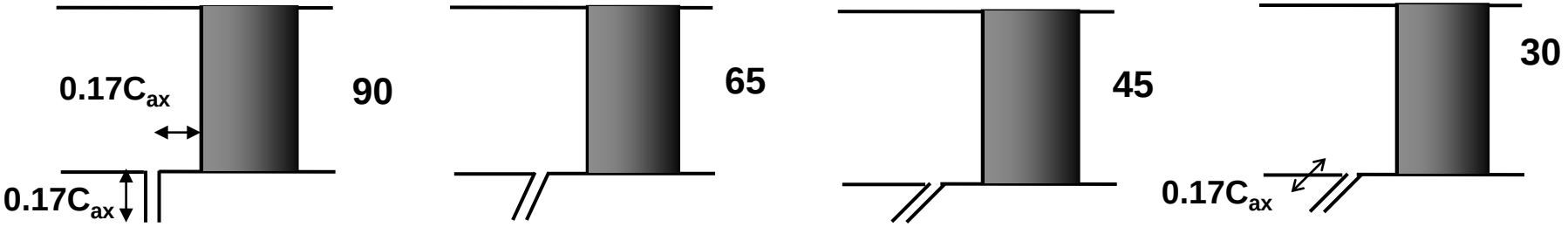

Net heat flux reduction characterized the durability of the vane endwall for leakage MFR and I

$$NHFR = \frac{q''_o - q''_c}{q''_o} = 1 - \frac{h_o}{h_c}\left(1 - \frac{\eta}{\varphi}\right)$$

$$\eta = \frac{T_\infty - T_{aw}}{T_\infty - T_c}$$

$$\varphi = \frac{T_\infty - T_w}{T_\infty - T_c}$$

overall effectiveness (metal temperature), assumed uniform value of 0.6

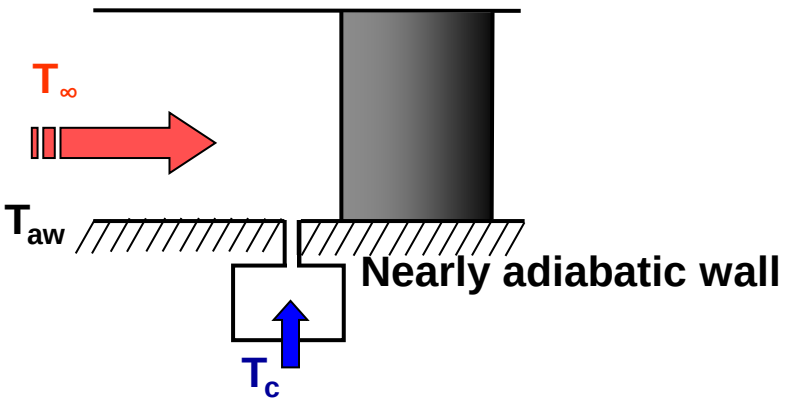

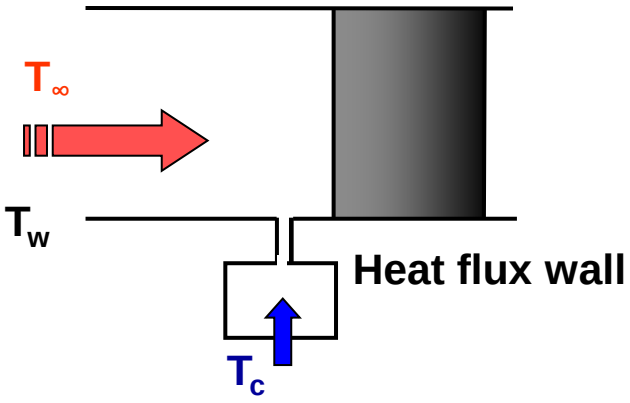

$$\text{mass flux ratio (MFR)} = \frac{\dot{m}_c}{\dot{m}_\infty}$$

$$\text{momentum flux ratio (I)} = \frac{\rho_c U_c^2}{\rho_\infty U_\infty^2}$$

The stagnation plane flow field was measured using a high-image-density TRDPIV system

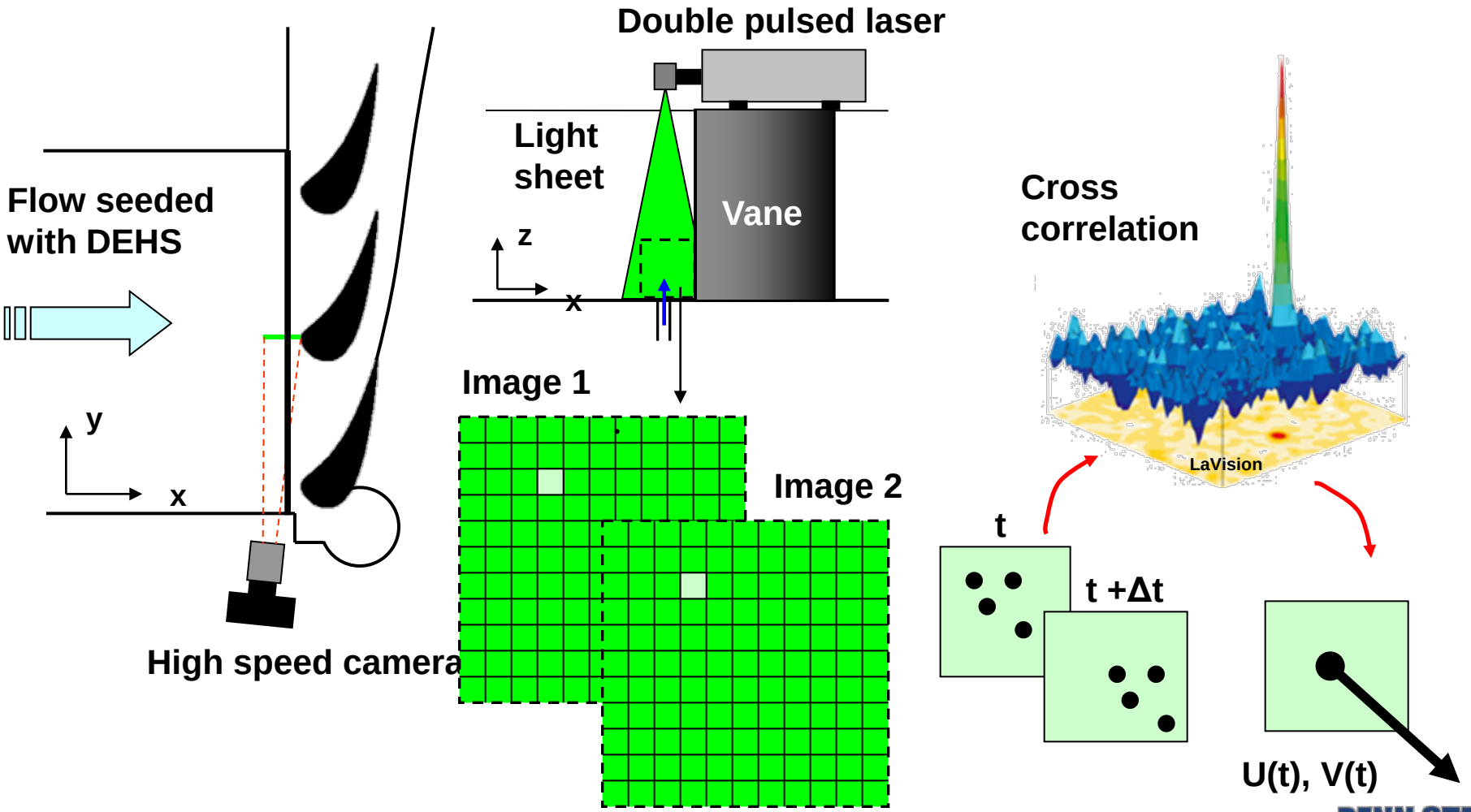

$t_1^* = \delta/U_\infty$

Flowfield was sampled at 1000Hz($12t_1^*$) for $250t_1^*$

The pressure side of the passage remains uncooled for all injection angles at low MFR

MFR = 0.5%, I = 0.7

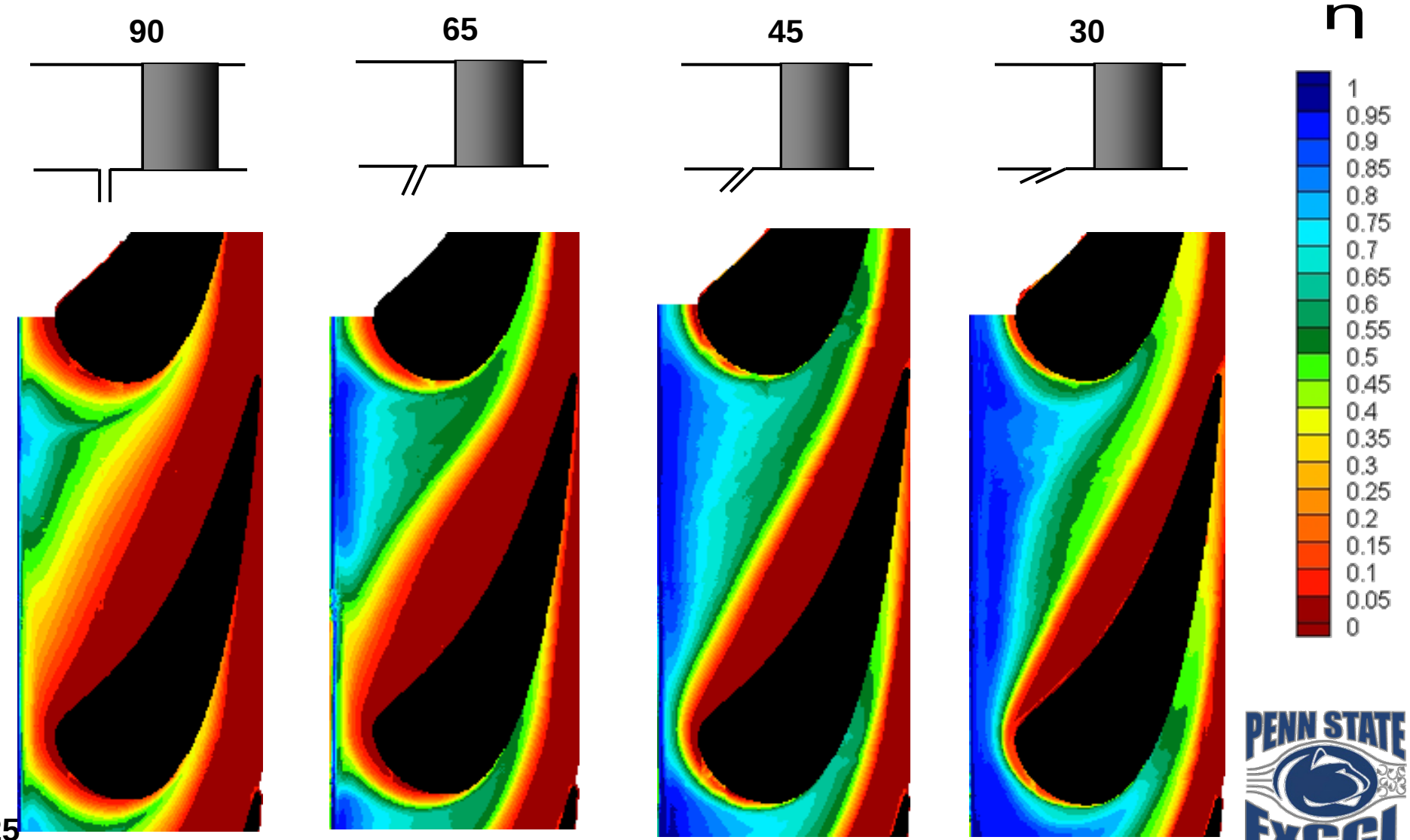

As injection angle was decreased, endwall effectiveness improved for higher MFR

MFR = 1.0%, I = 2.8

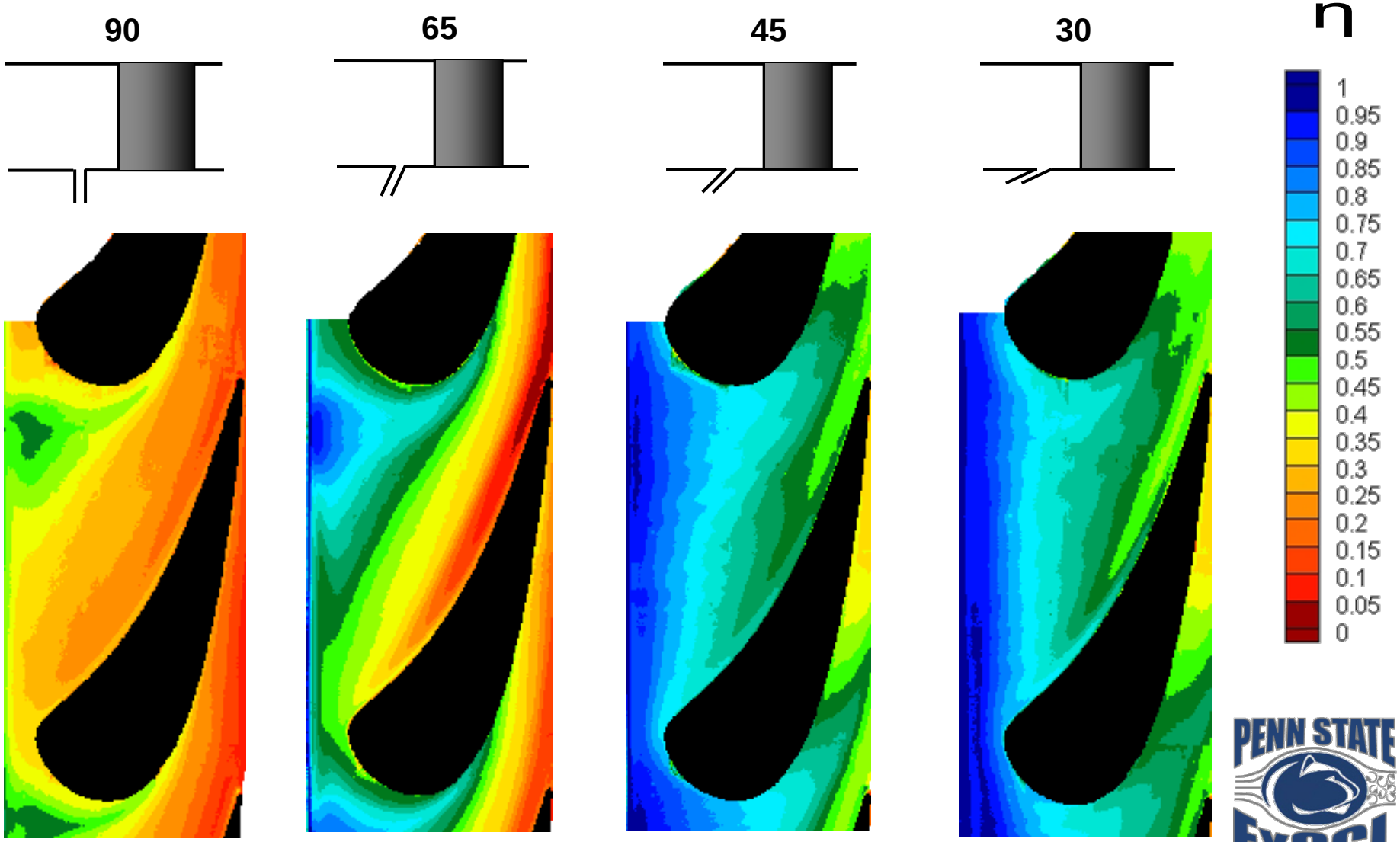

Nusselt number contours are less affected by slot orientation at the case with lower MFR

MFR = 0.5%, I = 0.7

$$Nu = \frac{h_c C_{ax}}{k_{air}}$$

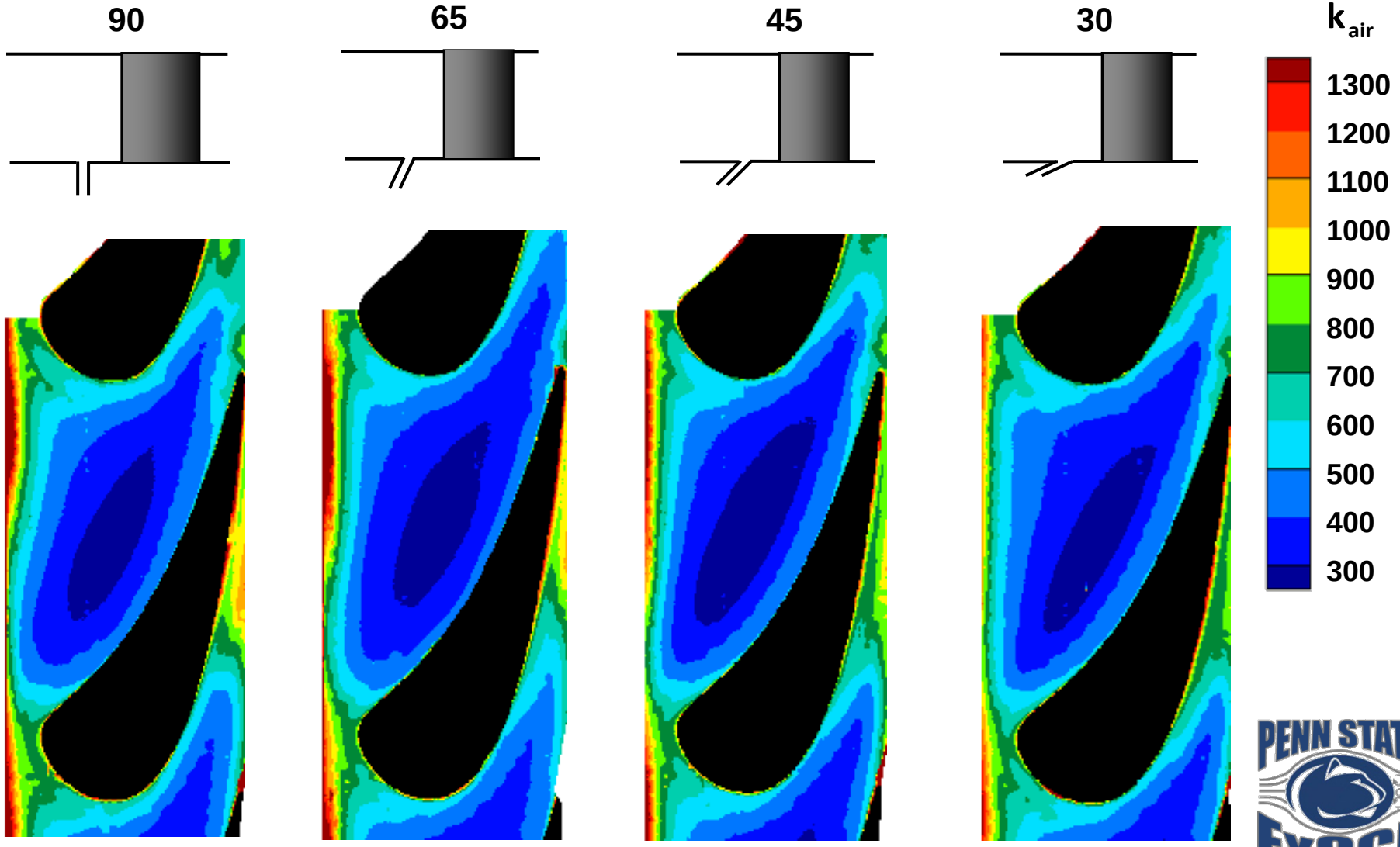

Nusselt number contours for orientation angles less than 45° had a more pitchwise uniform distribution

MFR = 1.0%, I = 2.8

$$Nu = \frac{h_c C_{ax}}{k_{air}}$$

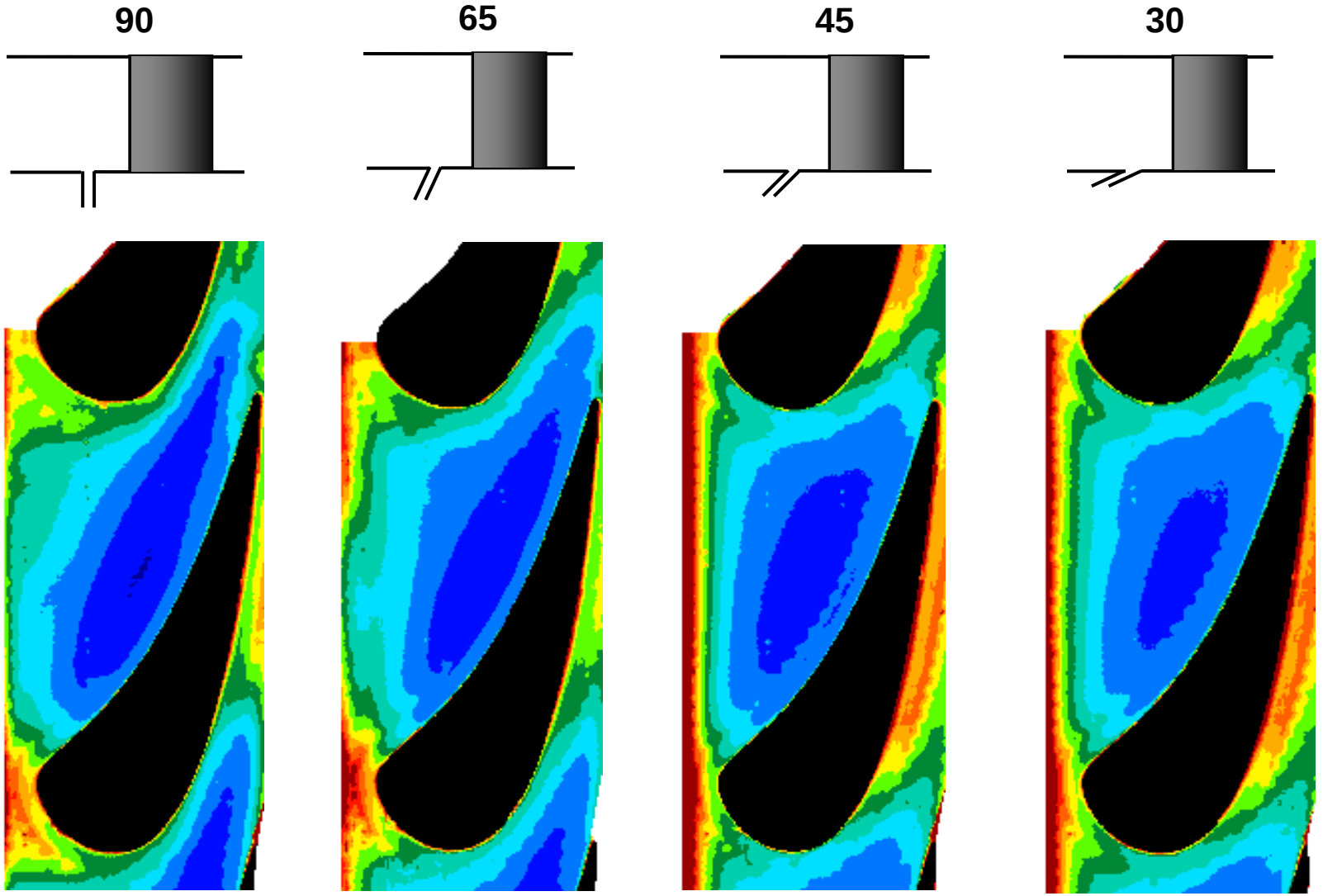

NHFR contours were mostly influenced by adiabatic effectiveness

$$NHFR = 1 - \frac{h_o}{h_c}\left(1 - \frac{\eta}{\varphi}\right)$$

MFR = 0.5%, I = 0.7

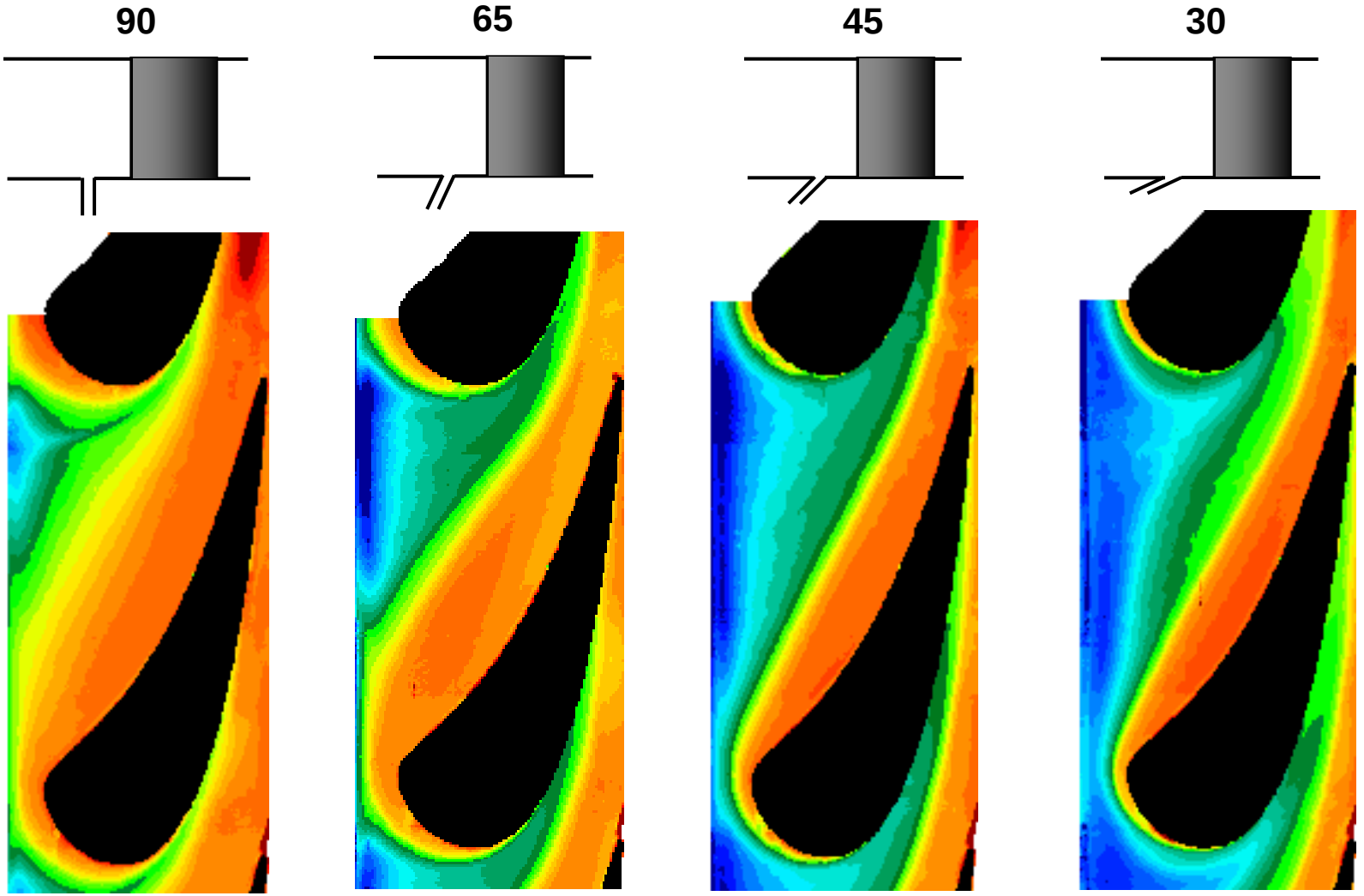

High momentum flux ratio results indicated most of the passage had a positive benefit from the slot

$$NHFR = 1 - \frac{h_o}{h_c}\left(1 - \frac{\eta}{\varphi}\right)$$

MFR = 1.0%, I = 2.8

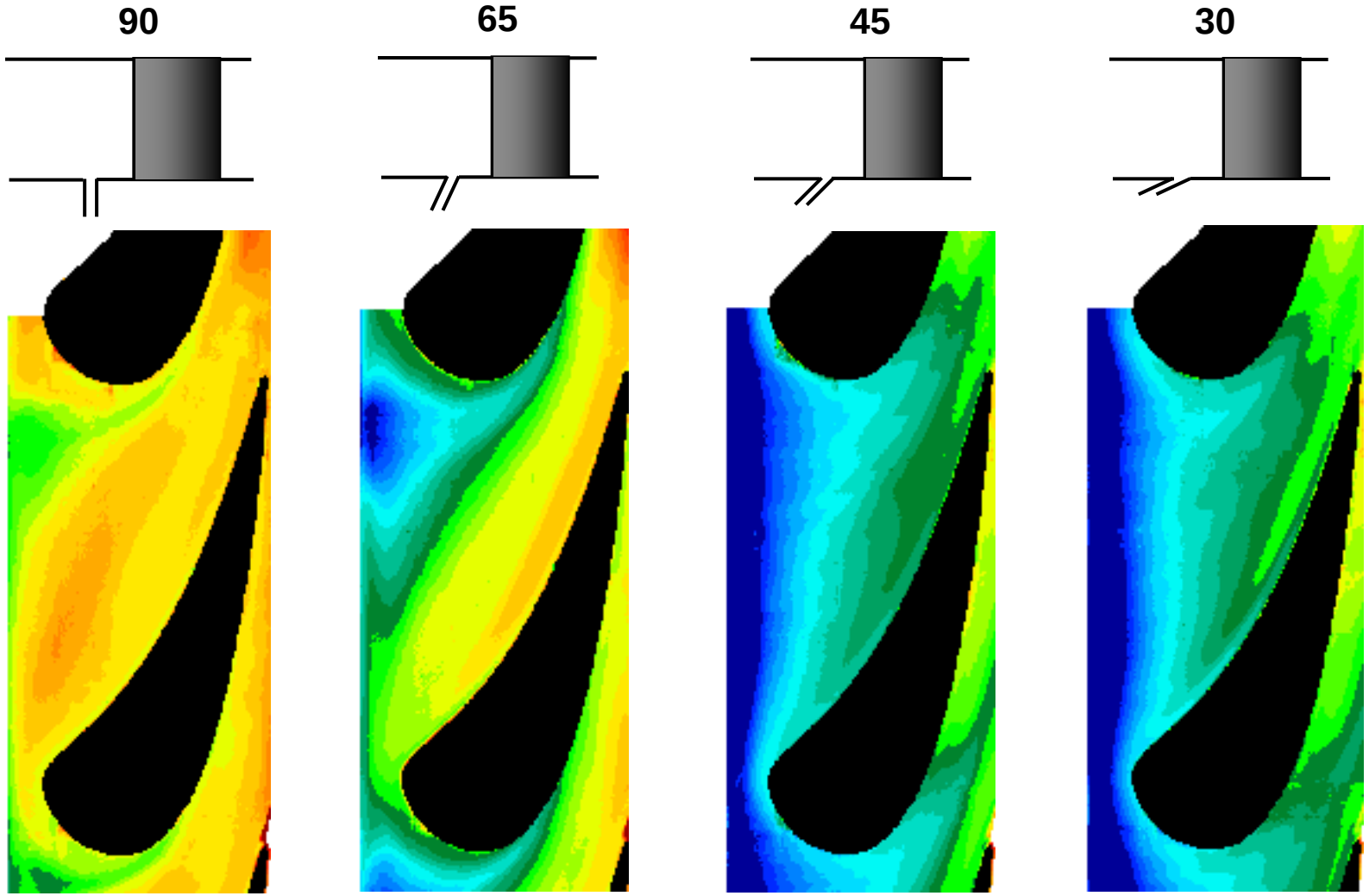

The highest area averaged net heat flux reduction was measured for I = 2.8, MFR = 1.0%, with a 45° slot

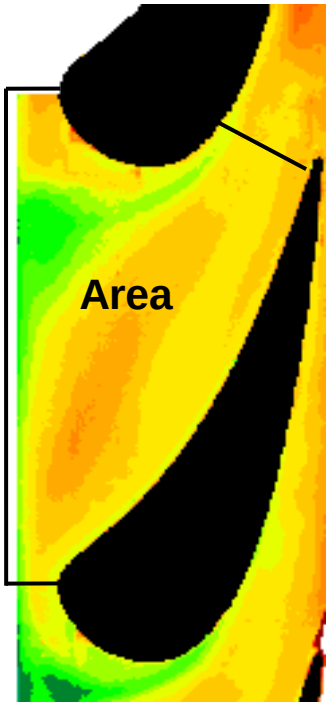

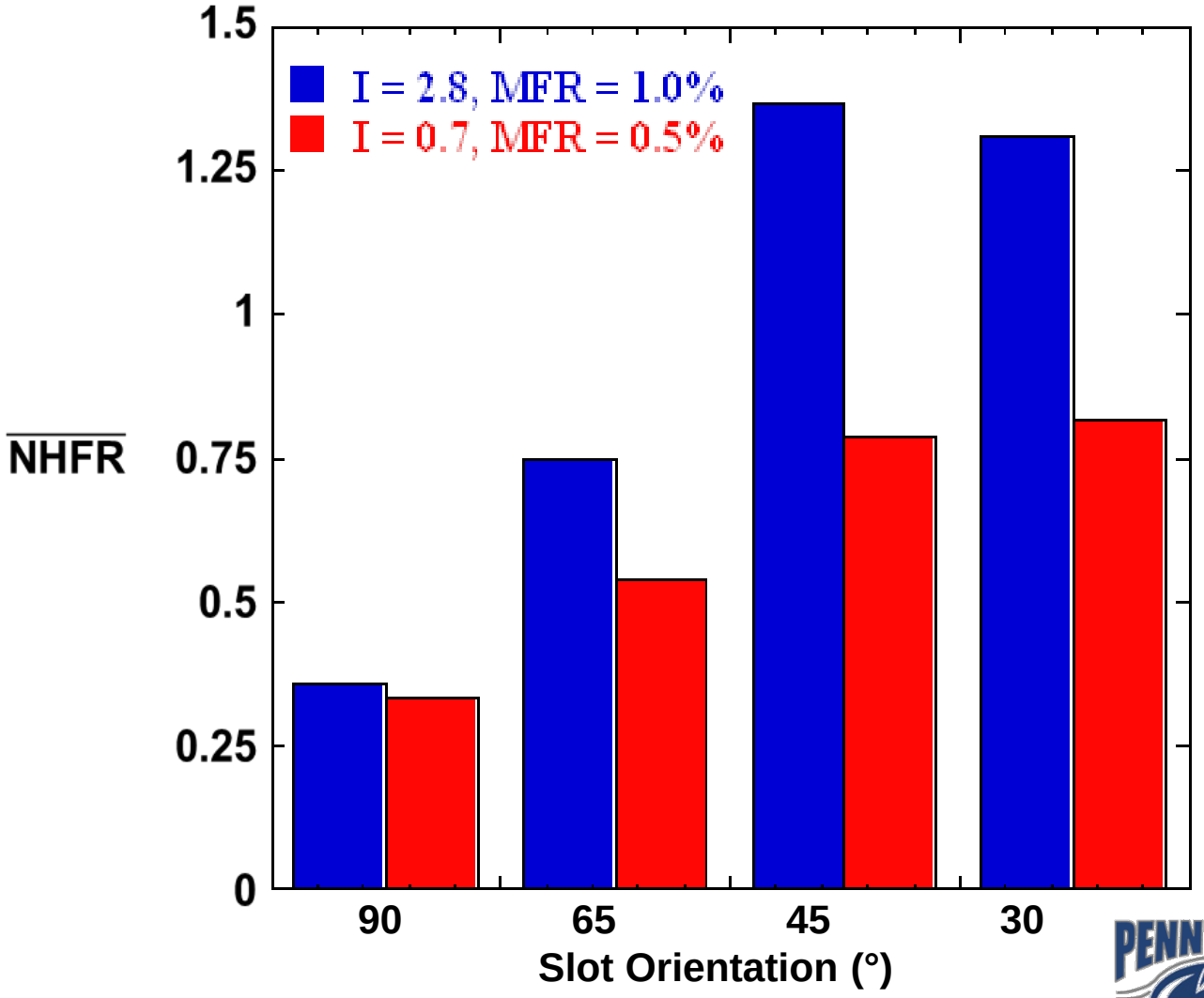

Cooling of the vane endwalls is complicated by secondary flows originating in the boundary layer

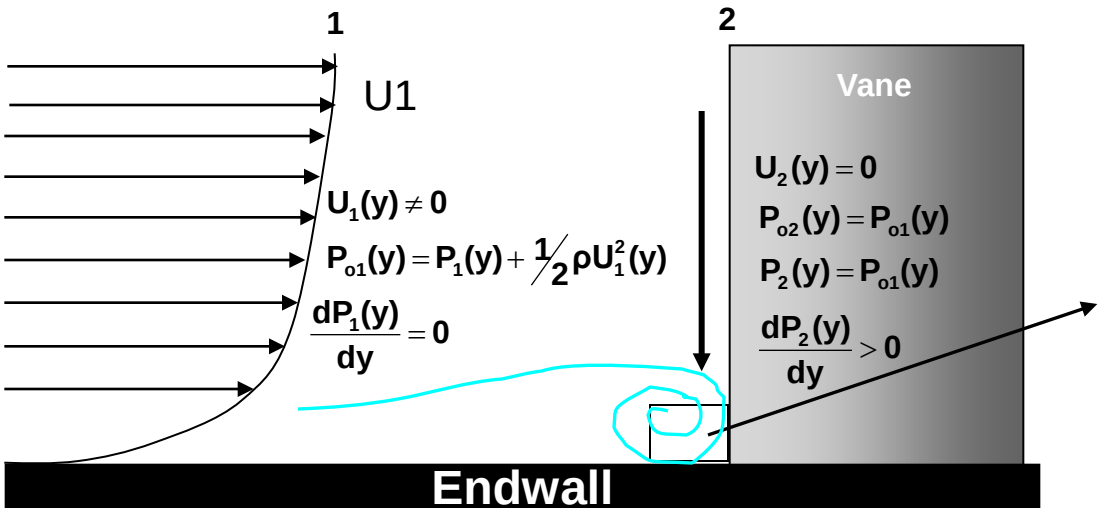

Horseshoe vortex

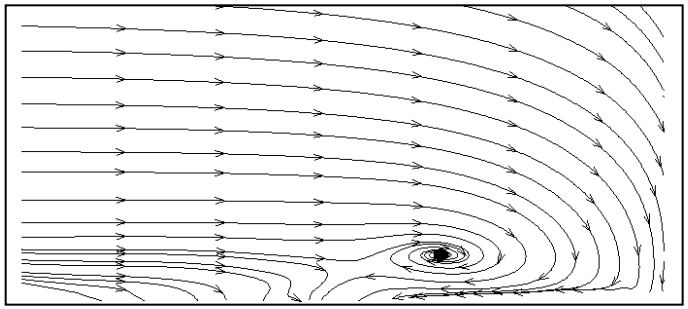

$$\left(\frac{\partial p}{\partial n}\right)_A = \frac{\rho_A U_A^2}{R_A} \qquad \left(\frac{\partial p}{\partial n}\right)_B = \frac{\rho_B U_B^2}{R_B}$$

$$\left(\frac{\partial p}{\partial n}\right)_A = \left(\frac{\partial p}{\partial n}\right)_B$$

The viscous layer ensures that UA > UB , therefore

$$R_A > R_B$$

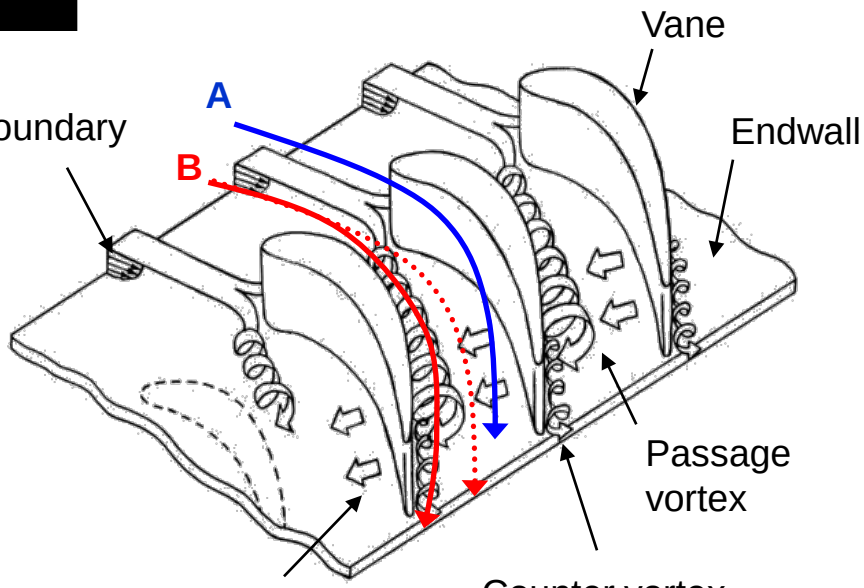

[Langston, 1980]

Far from the vane an elongated HSV was measured, close to the vane the HSV was smaller

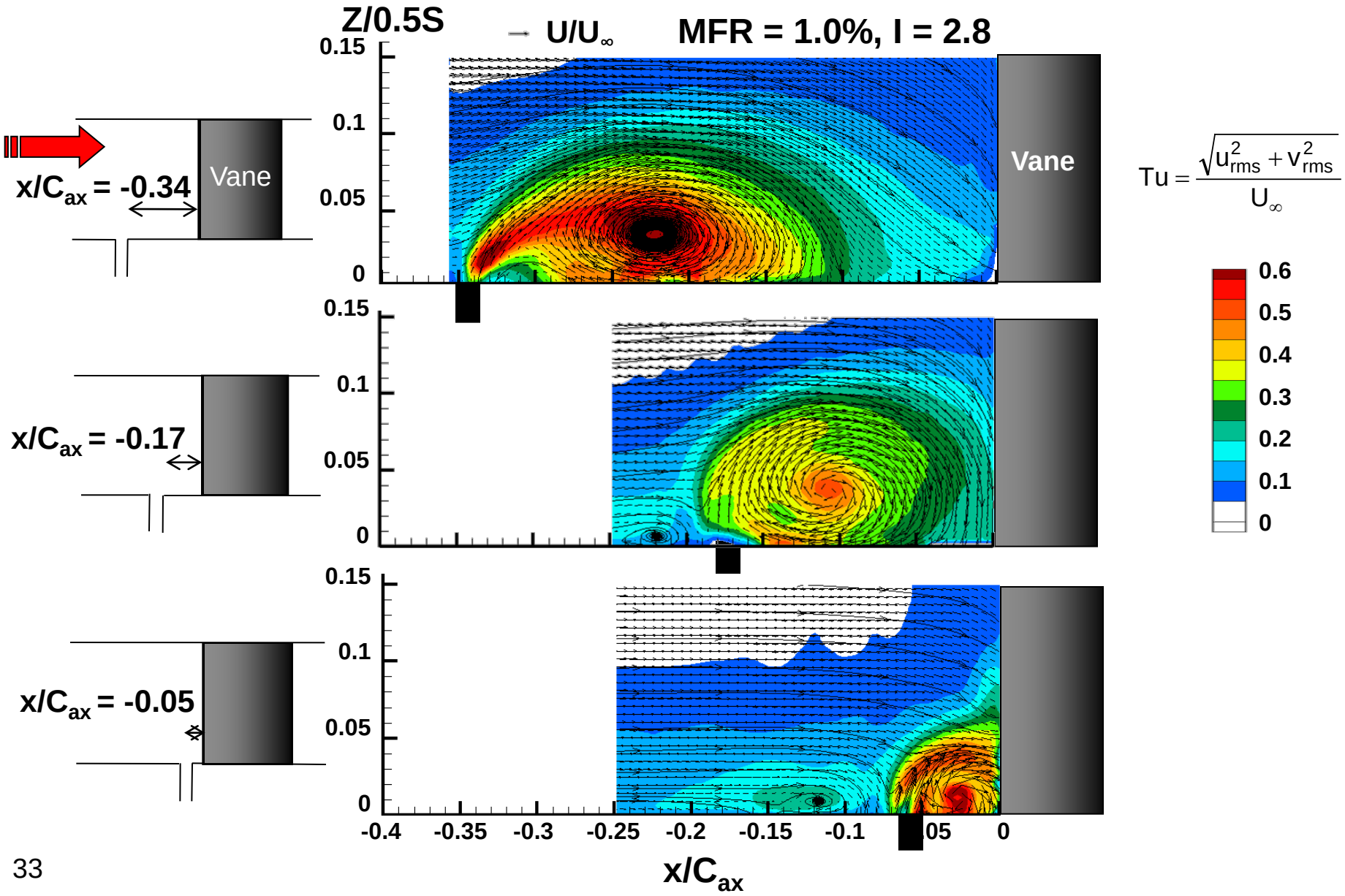

Intensity of the flowfield phenomenon increased with an increase in the MFR and I

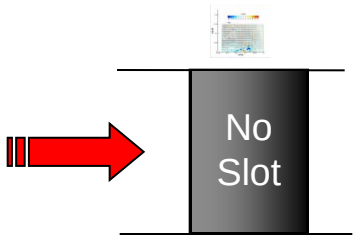

MFR = 1.0%, I = 2.8

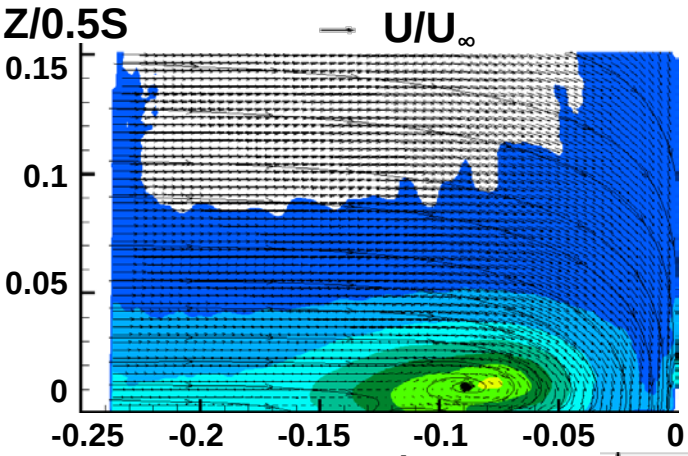

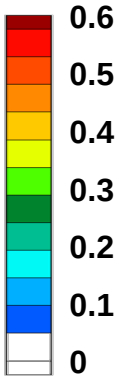

$$Tu = \frac{\sqrt{u_{rms}^2 + v_{rms}^2}}{U_\infty}$$

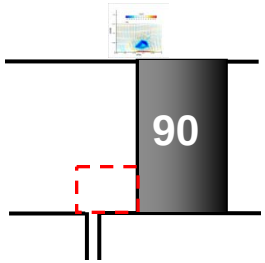

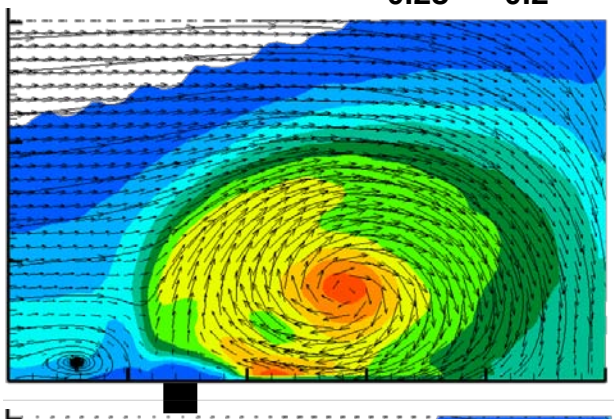

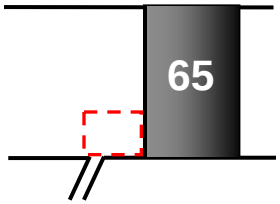

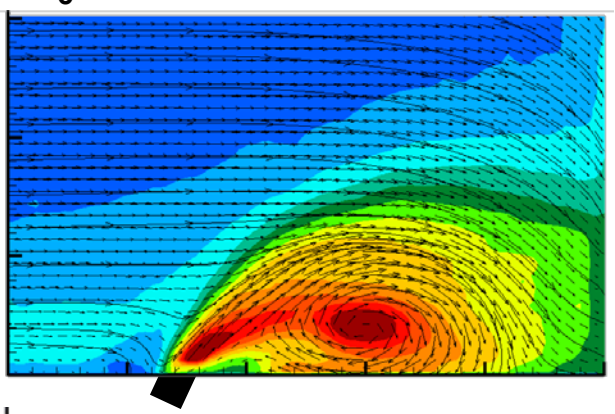

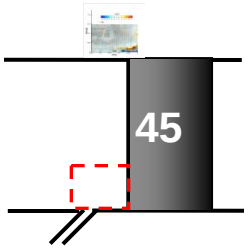

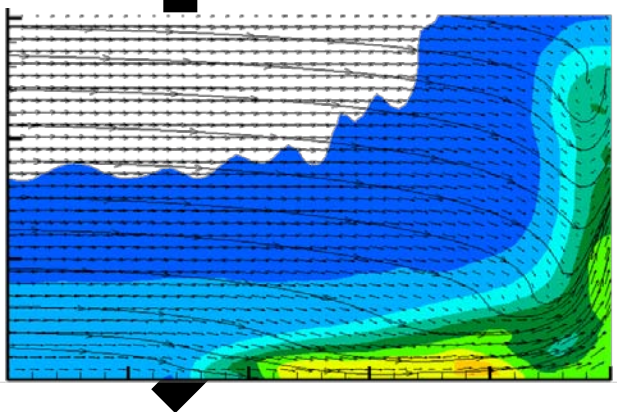

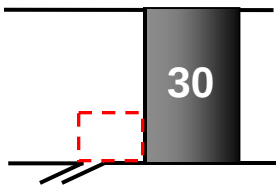

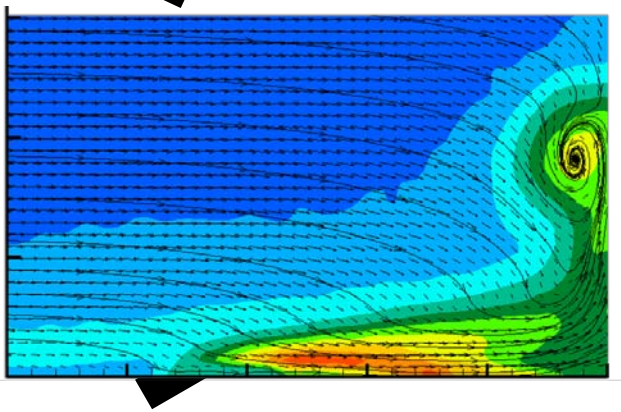

Flow injection increased turbulence, but reducing the slot orientation to 45 reduced the HSV

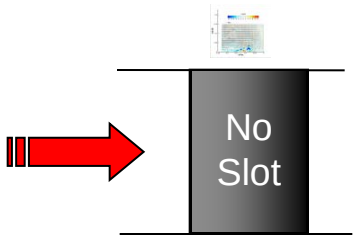

MFR = 0.5%, I = 0.7

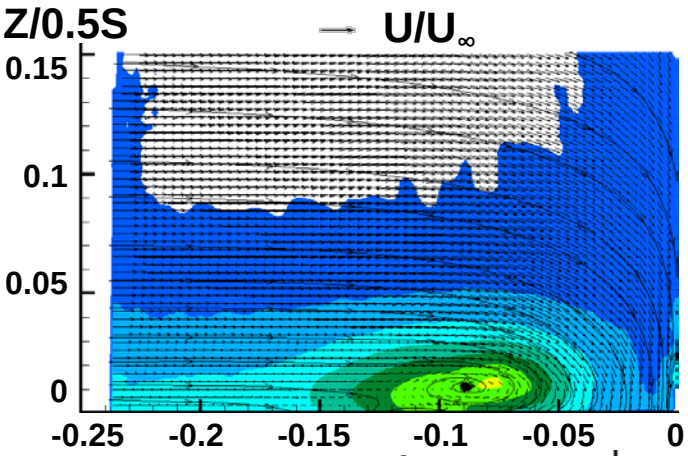

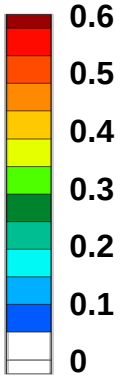

$$Tu = \frac{\sqrt{u_{rms}^2 + v_{rms}^2}}{U_\infty}$$

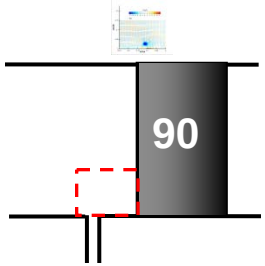

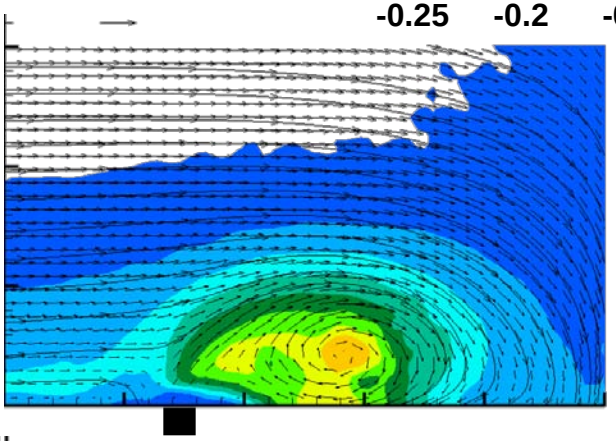

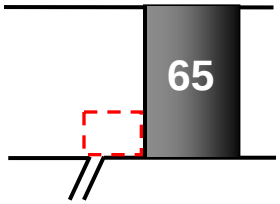

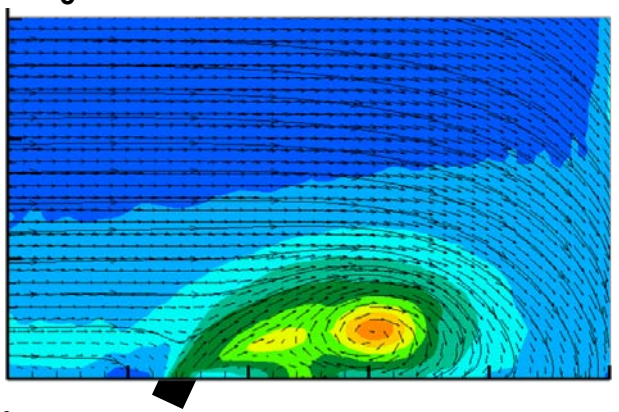

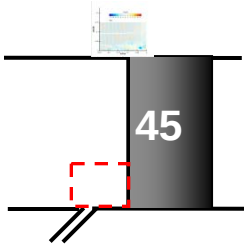

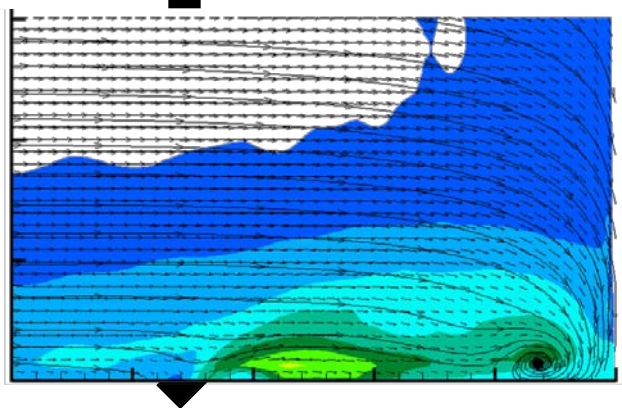

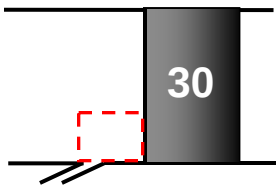

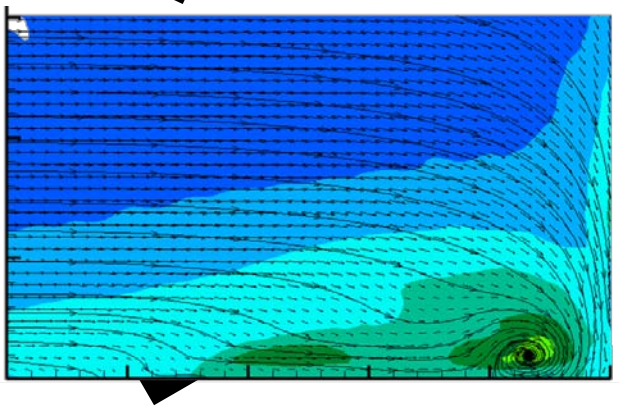

An oil flow visualization technique was used to draw streaklines of the flow along the endwall

Pack-B Blade Cascade

No. of airfoils	7
Scale	8.6x
Axial chord (C_{ax})	0.218 m
Pitch/chord (P/C_{ax})	0.89
Aspect ratio (S/C_{ax})	2.5
Exit Reynolds number	200,000
Exit Mach number	0.04
Zweifel loading coefficient (Z)	1.15

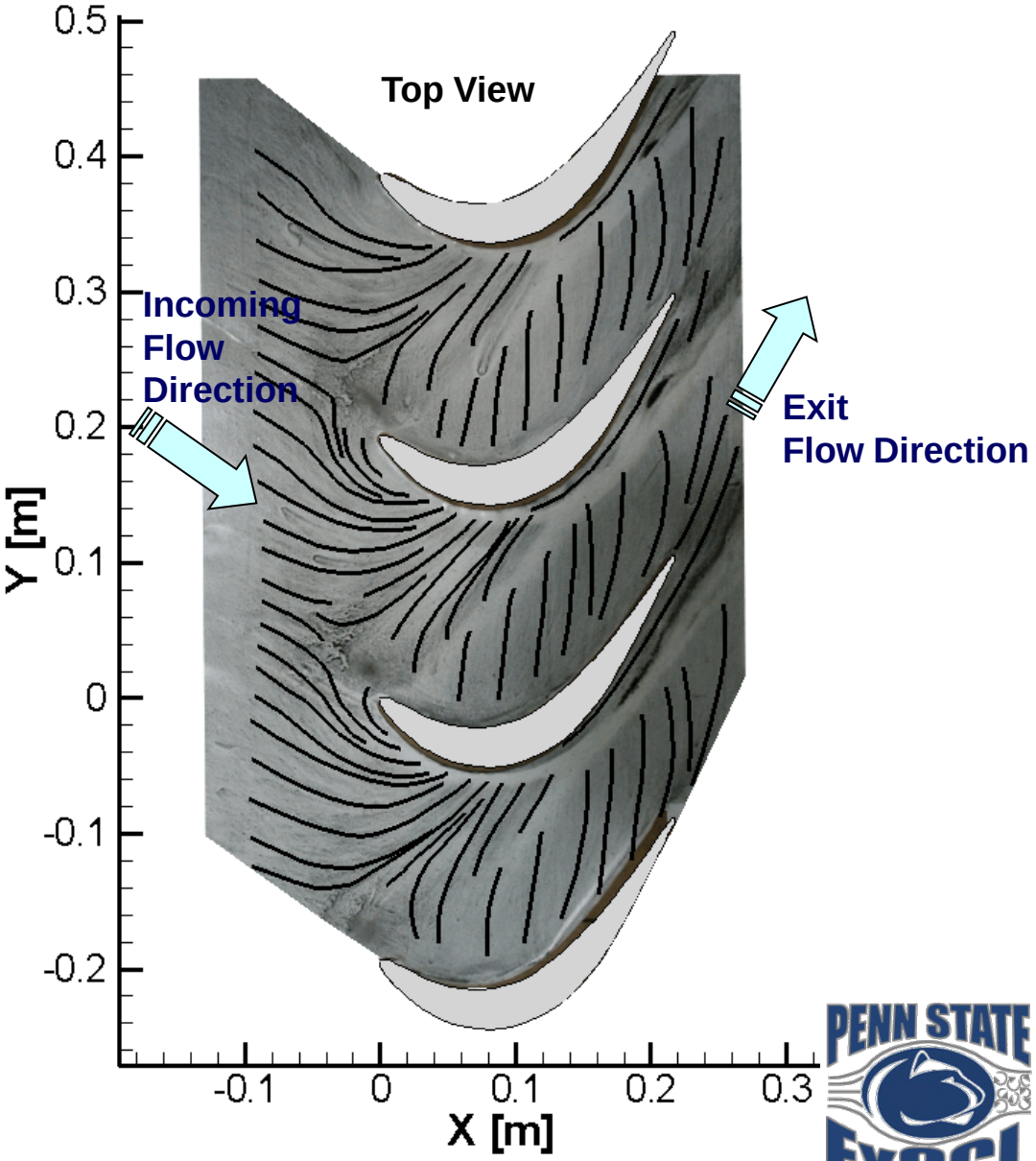

Conjugate heat transfer effects can be modeled by matching endwall Bi and h_o/h_i to engine parameters

$$\text{Overall effectiveness, } \phi = \frac{T_\infty - T_{wall}}{T_\infty - T_c} = \frac{\eta - 1}{1 + Bi + h_\infty / h_i} + \eta$$

$$Bi = h_\infty t / k_{wall}$$

$$\eta = \frac{T_\infty - T_{aw}}{T_\infty - T_c}$$

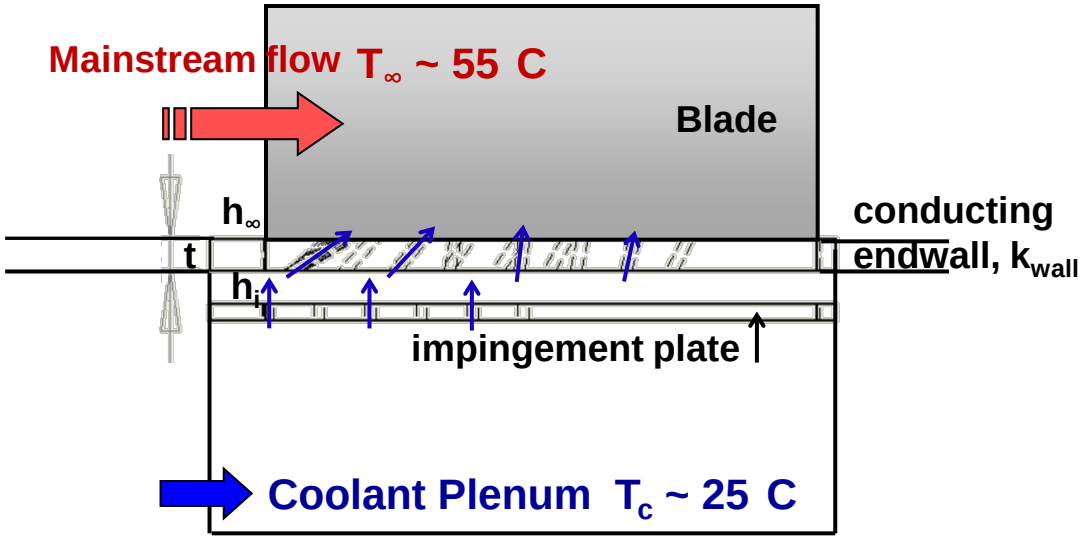

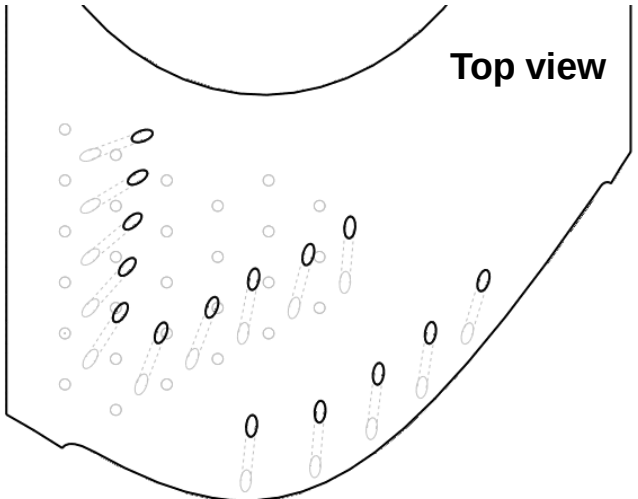

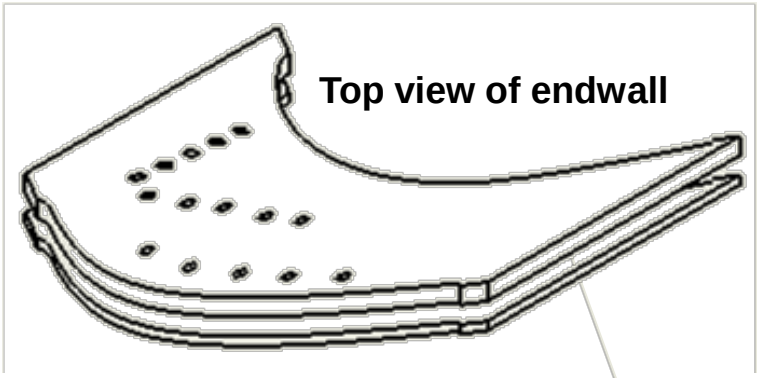

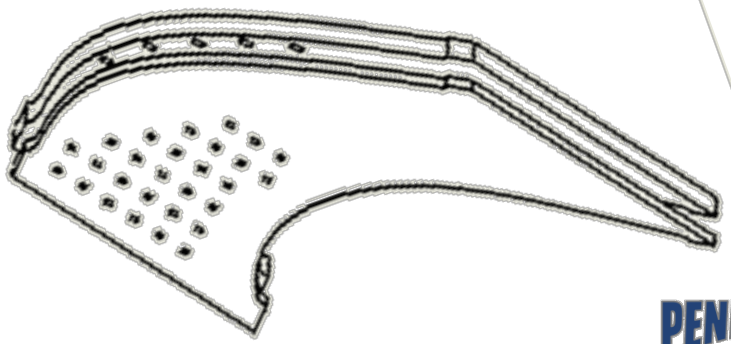

Bottom view of impingement plate

Conclusions

Measurements of the overall cooling effectiveness show the relative benefits of TBC and film cooling.

Cooling benefit of TBC dominated to the extent that there will little effect of the improved film cooling from crater and trench configurations.

Ironically the insulating effect of simulated depositions improved overall cooling effectiveness.

Reducing the angle below 45 for high momentum injection improved endwall cooling effectiveness.

Coolant injected at the lower momentum flux ratio was unable to cool the pressure side of the passage.

Questions?

Background image: [Hamed, A., Tabakoff, W., and Wenglarz, R., 2006]